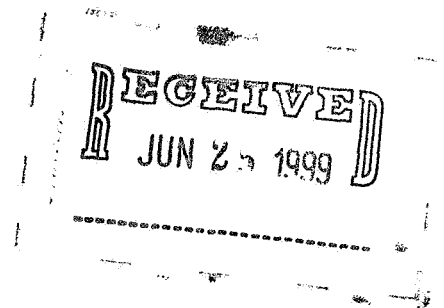


399279  
50pGRANT  
IN-34  
1/2 3/8

**Final Report  
for  
Numerical Study of Tip Vortex Flows**

Jennifer Dacles-Mariani  
Mohamed Hafez  
Mechanical and Aeronautical Engineering Dept.  
University of California, Davis



NASA Co-op Agreement NCC2-873

Aug 1, 1997- July 31, 1998

recd.  
JUN 17 1999

CC:202A-31

CASI

## **OUTLINE**

### **1.0.0 Introduction**

### **2. 0.0 Analytical Vortices**

#### **2.1.0 Laminar Vortices**

#### **2.2.0 Turbulent Vortices**

#### **2.3.0 Other Related Analytical Studies**

### **3.0.0 Experimental Studies**

#### **3.1.0 Formation and Roll-Up Process (With Turbulence Measurements)**

#### **3.2.0 Near-Wake Flowfield (No Turbulence Measurements)**

#### **3.3.0 Near and Intermediate-Wake Flowfields ( With Turbulence Measurements).**

#### **3.4.0 Far Wake**

### **4. 0.0 Computational Studies**

#### **4.1.0 Formation and Roll-Up Process/Near-Wake (With Turbulence Measurements)**

#### **4.2.0 Near-Wake/Turbulence/Engine Exhaust Interaction**

#### **4.3.0 Intermediate- and Far-Wake**

### **5.0.0 Wake Vortex Control and Management**

#### **5.1.0 Experimental Studies**

#### **5.2.0 Computational Studies**

### **6.0.0 Wake Modeling**

#### **6.1.0 Modeling Techniques**

#### **6.2.0 Wake Vortex and Ground Interaction**

#### **6.3.0 Wake Vortex with Atmospheric Modeling**

6.4.0 Wake Vortex Pair Interaction

## **7.0.0 High-Lift Systems**

7.1.0 Experimental Studies

7.2.0 Computational Studies

## **8.0.0 Issues in Numerical Studies**

8.1.0 Spatial Order of Differencing Scheme

8.2.0 Transition/Turbulence Modeling

8.3.0 Outflow Boundary Condition

8.4.0 Adaptive Gridding

## **9.0.0 Instabilities**

9.1.0 Crow Instability and Small Scale Instabilities

9.2.0 Vortex Breakdown

## **10.0.0 Related Topics**

10.1.0 Rotorcraft Vortex Wakes

10.2.0 Tip Vortex Leakage in a Linear Cascade Turbine

10.3.0 Ship Propeller Blade Cavitation

## **11.0.0 Visualization Tools for Vortical Flows**

## **12.0.0 Further Work Needed**

## **13.0.0 Acknowledgments**

## **14.0.0 References**

## **15.0.0 Appendix**

15.1.0 Characterization of Wake Vortex Flows

## **SUMMARY**

This paper presents an overview and summary of the many different research work related to tip vortex flows and wake/trailing vortices as applied to practical engineering problems. As a literature survey paper, it outlines relevant analytical, theoretical, experimental and computational study found in literature. It also discusses in brief some of the fundamental aspects of the physics and its complexities. Although it is not an exhaustive list, it is comprehensive enough to direct the reader to relevant issues and shortcomings being considered in this research area and more importantly it also presents unresolved issues that are considered important by some of the leading experts in the field. The reader is referred to a recent paper by Spalart (1997) for a detailed survey of the formation, motion and persistence of trailing vortices. He provides specific attention on the relevance of the studies to the safety and productivity of air travel.

### **1.0.0 INTRODUCTION**

The wingtip vortex flow has been the subject of numerous studies. Its significance has been seen in practical engineering problems such landing separation distance for aircraft, blade-vortex interaction and cavitation on ship propeller blades. Despite these numerous studies, a full understanding of the wake vortex flow in its entirety, i.e., roll-up and formation on a lifting surface to its growth, convection and decay in the wake region, is still not clearly understood. A major contribution factor to this is the fact that trailing vortices can persist for several miles downstream of a lifting surface. As it travels downstream, it undergoes several physical changes which are complicated and not well understood.

The roll-up and formation of the tip vortex occur on the tip of the lifting wing of finite span. Close to the tip, a pressure differential exists between the upper and lower surfaces which drives the fluid around the tip from the high pressure side on the lower surface to the low pressure side on the upper surface. The fluid becomes highly three-dimensional as it undergoes thorough this motion. The vortex then moves downstream and rolls up more and more of the wing wake until its circulation is nominally equal to that of the wing. This roll-up distance is found to be small compared to separation distances of aircraft on the approach path. However, it is not necessarily small when compared to distances between interacting lifting surfaces, ( i.e., the strake or foreplane and the main wing on a closely-coupled fighter aircraft and the flow on consecutive rotor blades of a helicopter). Thus, the flow around the wingtip and the near-field is important. It is also relevant to study in that it can provide some possible means of controlling the far-field vortex behavior. Computationally, this proves to be a challenging flowfield to study because of the presence of turbulence and the large gradients of pressure and velocity in all three direction.

In the near-wake region, the tip vortex continues and completes its roll-up process. This typically extends to a few wing spans downstream of the trailing edge. On an aircraft configuration, the engine exhaust plumes interacts and affects the development of the vortex wake. More specifically, in the near field, the exhaust plumes will influence the for-

mation of the vortex cores. This interaction between the vortex wake and the exhaust gases occur and the condensation trails (contrails) are formed. The wake roll-up process will be completed before the exhausts and the wake begin to merge. As it travels downstream, the exhaust gets entrained in the vortex cores (Hoeijmakers, 1996).

The tip vortex is convected downstream and is typically called the wake or trailing vortex. The downstream region can be further divided into two regions. The intermediate-wake region typically extends to a few hundred wing spans while the far-wake region happens at a distance greater than a few hundred wing spans. Most, if not all of the wake vortex study has been focused in these regions. Some added complexities at this stage include instabilities in the flow occurring such as Crow instability or vortex burst/breakdown, interaction of the vortex pair with each other or with the ground, and atmospheric conditions including ambient turbulence, wind and stratification.

Another area of great concern is wake vortex control and management. This is also typically called wake hazard alleviation and avoidance of wake vortex encounters. In the early 1970's, this has been a topic of great concern. To date, most of the attempts to reduce the hazard of the vortex wake of the generating aircraft without affecting the performance of the aircraft itself remain unsuccessful.

Finally, there is a need to improve flow visualization of vortical flows. This may prove to be essential in tracking down flow areas of interest in an automated fashion on large computational data sets. These features may include, locating the vortex core of a tip vortex or the onset of vortex burst/breakdown.

## **2.0.0 ANALYTICAL VORTICES**

Tip vortex studies have generally been more successful in the far-field than in the near-field. The simplifying assumptions made in the far-field analysis may not hold in the near-field. The main assumption in all previous analytic studies is that of axisymmetric flow. In the early stages of roll-up, this is not a good assumption. Other assumptions that are often made are that the axial velocity perturbation is small with respect to  $U_{inf}$  (light loading) and that the apparent eddy viscosity is isotropic. In the near-field both of these conditions do not hold. However, these analytical vortices have been successful in predicting the far-field behavior of the vortex.

### **2.1.0 Laminar Vortices**

The simplest analytic model for a 2-D line vortex assumes solid body rotation of a viscous core surrounded by an irrotational field. This is a simple approximation to the well known solution for the growth of a laminar 2-D line vortex which can be found in Lamb (1932). In 1964, Batchelor did an analysis on axial flow in a laminar trailing vortex starting with the steady axisymmetric incompressible momentum equations. The equations show that as the roll-up of the vortex generates larger and larger tangential velocities, pressure forces produce a strong downstream flow in the core of a trailing vortex, pro-

vided only that the total head losses are not large. Similarly, as the tangential velocities decay in the far-field part of the flow, pressure forces will act to decelerate the axial flow in the core.

**Moore and Saffman** (1973) sought to improve upon Batchelor's analysis and studied the influence of viscosity on the axial flow in a laminar trailing vortex. They noted that although Batchelor's primarily inviscid arguments suggested a large axial velocity excess 'wind tunnel tests and free-flight observations show that there is usually a deficit of axial velocity in the core, although some cases of a velocity increase have been reported'. Using a light loading approximation, their solution of a semi-infinite rectangular wing gives two different axial profiles for the vortex centerline. Comparisons with available experimental data are poor although the measurement of Logan (1971) showed a qualitatively similar axial flow. Although their analysis is claimed to be valid for the near-field, the assumptions made in the analysis (axisymmetric, light loading, laminar boundary layers) make comparisons to near-field experimental data difficult.

**Burgers**(ref) has discussed an exact solution of the Navier-Stokes equations for a three-dimensional viscous vortex. Also, **Rott**(ref) considered the same solution in more detail which includes an extension of the tangential velocity varying with time and determining the distribution for the temperature and pressure. Here the solution is recognized as potential flow and so an exact solution of the Navier-Stokes equations. The radial and vertical velocities are components of an axisymmetric stagnation-point flow; if the velocity gradient is positive, the radial flow is directed inward toward the z-axis. Then superimposed is a potential vortex with the circulation centered around the z-axis.

An analog to Burgers solution with two cells has been found by **Sullivan** (1959) in which  $u$  and  $v$  are functions of  $r$  only and  $w$  is a function  $rz$ . By two cells is meant that the flow does not simply spiral in toward the axis and out along it. It has a region of reverse flow near the axis. Note that this flow for large  $r$ , corresponds to the once-cell (Burgers vortex) case. Several deficiencies in Sullivan's solution is noted. First, there is no coupling between  $v$  and the  $u, w$  field. This is due to the assumption of the forms of  $u$  and  $w$  at the outset. As a consequence of this lack of coupling between the tangential and flow-though fields, the model is limited in its ability to properly respond to changes in background conditions. Also the viscosity is taken to be constant throughout the flow. However, it does incorporate some of the essential physics of actual two-celled vortices. In particular, the role of the downdraft along the centerline in creating the central pressure is brought out. Also, the overall progression of the shape of the radial profile of the wall static pressure on the lower surface as the input angular momentum is increased is qualitatively reproduced.

A class of self-similar solutions of the steady, axisymmetric Navier-Stokes equations for flows in slender vortices are presented by **Mayer and Powell** (1992). The effects of vortex strength, axial gradients and compressibility are studied. They show that the presence of viscosity couples the core growth rate and the external flowfield. The numerical solutions also show that the presence of axial pressure gradient has a strong effect on the axial flow in the core. In the case of the viscous compressible vortex, non-zero densi-

ties and pressures and low temperatures are seen on the vortex axis as the strength of the vortex increases. They also show that compressibility has a significant influence on the vorticity distribution in the vortex core. Another study which dealt with the effect of compressibility on free (unsteady) viscous heat-conducting vortices is the work done by **Colonius, Lele, and Moin (1991)**. They found analytical solutions in the limit of large but finite Reynolds number and small but finite Mach number. Their analysis show that the spreading of the vortex causes a radial flow. They compare with the experiments by **Mandela (1987)** which report a radial flow in the vortex, but their estimates are much larger than the analytical predictions. It is speculated that the three-dimensionality effect is the cause of this discrepancy. The analytical solutions show that the swirling axisymmetric compressible flows generate negative radial velocities far from the vortex core due to viscous effects regardless of the initial distribution of vorticity, density and entropy.

In the analysis of the intermediate-wake region, current studies use the wake definitions of theoretical vortices to prescribe the vortex wake structure and test the accuracy of the models. At this point, the flow is inviscid and convects without too much of diffusion. These include the Rankine vortex, Lamb vortex, extended Lamb vortex and Perturbation vortex, and the Betz rollup structure from a given span loading(Ref). These vortices were considered as candidates because they satisfy several conditions. One of them is that the circumferential or swirl velocity must have zero velocity at the vortex core center. Further, the velocity far from its center should decrease as the inverse of the core radius. **Roscow et al (Ref)** in his study of wake-vortex structure found that the Lamb and perturbation vortex structures gave smoothly contoured profiles which match the ranges of shapes of the measured vortex wake. The pointed shape of the Rankine vortex at the edge of the core trends to always give a mismatch. In the extended Lamb vortex model he used, it has an extra term in the exponent which was found to give difficulty at small radii. The use of a vortex profile derived by Betz was found to be a good idea for a basic profile on which perturbations could be placed. However, the Betz' structure usually have an infinite velocity at their center because the span loading has an infinite gradient at the wing tip.

## 2.2.0 Turbulent Vortices

Past analytical studies done on a turbulent tip vortex have assumed isotropic eddy viscosity to represent the behavior of turbulence. **Squire's (1954)** analysis of a turbulent line vortex augmented the laminar viscosity by a turbulent eddy viscosity whose value was proportional to the total circulation. The analysis by **Hoffman and Joubert (1963)** on a turbulent line vortex predicted a constant eddy viscosity and a logarithmic radial variation of circulation in regions where the inertial forces in the tangential momentum equation are small in comparison to the Reynolds stresses.

**Govindaraju and Saffman (1971)** predicted an overshoot of circulation for a fully rolled-up turbulent vortex under light loading. However, convincing experimental evidence of the existence of an overshoot of circulation is lacking.

In 1974, **Lezius** noticed that in towing tank tests between 100 to 1,000 chords downstream of an airfoil set at 8 degrees, the vortex decayed at a rate proportional to  $t^{-7/8}$ , not the usually predicted  $t^{-1/2}$ . The towing tank tests had  $Re_c$  ranging from  $2.2 \times 10^5$  to

7.5x10<sup>5</sup>. It was reasoned that the increased decay rate was due to turbulence that had not yet reached equilibrium.

**Phillips (1981)** analyzed the near-field roll-up of a turbulent vortex. With the exception that the boundary layers were considered to be initially turbulent, the analysis was similar to that of Moore and Saffman, with the same assumptions of light loading and axisymmetry of the vortex core.

### **2.3.0 Other Related Analytical Studies**

The influence of spanwise lift-tailoring on the stability of vortex roll-up was studied in 1991 by **Lezius**. He used Rayleigh's stability criterion for a two-dimensional vortex and reasoned that a lift distribution which created a radially decreasing circulation at some point would create an instability in the roll-up and so increase the rate of decay of the velocities. Small scale experimental studies were done which qualitatively demonstrated the validity of the idea.

**Widnall and Wolf (1980)** analytically studied the effect of the tip vortex structure on helicopter noise due to blade-vortex interaction. Under certain flight conditions (usually descent), an impulsive noise called "blade slap" is generated at the blade passage frequency due to the passage of blade through the preceding blade's tip vortex. The sources of this impulsive noise have been thought to be due to two sources: shock formation due to local transonic velocities induced upon the flow wing blade; and unsteady lift fluctuations generated by the blade-vortex interaction. Their analysis is for incompressible flow which ruled out consideration of noise generated by the unsteady transonic velocities. The inviscid roll-up model of Betz was used to calculate the velocity profile in the vortex and the unsteady lift on the blades due to the blade-vortex interaction was calculated using linear unsteady aerodynamic theory. They concluded that substantial reduction in blade slap intensity could be obtained through the use of a tapered blade tip. More generally, varying the slope of the spanwise load distribution near the tip was found to greatly influence noise levels generated by the blade-vortex interaction.

## **3.0.0 EXPERIMENTAL STUDIES**

Tip vortex flows has been the subject of hundreds of experimental studies but concentrated mostly on the mean flow measurements in the far-field. The study of the near-field vortex rollup process detailed enough to be used for developing or testing a prediction method or for putting the design of tip modification on a firm fundamental basis is still being investigated. The lack of experimental studies in this area is related to the difficulty in measuring a highly turbulent flow with large gradients in all three directions near a curved solid body.

### **3.1.0 Formation and Roll-Up Process (With Turbulence Measurements)**

To date, the most detailed flow field analysis of the formation, roll-up and near-wake of the tip vortex is done by **Chow, Zilliac and Bradshaw. (1991)**. In their study, the complete mean flowfield and the complete Reynolds stress tensor have been measured in



the near-field of a turbulent vortex. Measurements of the mean flow and extensive turbulence statistics were made at data planes from 0.591 chords upstream of the trailing edge to 0.678 chords downstream of the trailing edge. They found that through this detailed study, they gained a better understanding of the initial roll-up process and also a better understanding of the behavior of the turbulence in the vortex in the near-field. Their measurements were detailed enough to show the existence of a primary vortex with a secondary vortex. They also found that the development of the crossflow velocities with chordwise distance induced a favorable axial pressure gradient in the vortex core which results in accelerating the core centerline fluid to 1.77 times the free stream velocity. Such high levels of mean axial velocity excess have not been measured previously in unswept wings.

### **3.2.0 Near-Wake Flowfield( No Turbulence Measurements)**

**Grow** (1969), performed near-field measurement of tip vortex flow for various wing shape parameters using a five-hole pressure probe and a vorticity meter. He found that 90% of the measurable circulation enters the tip vortices within one chord of the trailing edge. Later, **McCormick, Tangler & Sherrieb** (1968) reduced Grow's data to obtain some linear empirical formula for the maximum tangential velocity in the near-field at  $Re_c = 3.5 \times 10^5$ . In 1970, Spivey and Moorehouse showed a characteristic suction peak on the tip showing the approximate location of the primary vortex. In some occasion a second suction peak was found outboard and downstream of the primary peak which they attribute to be due to a secondary vortex.

**Orloff** (1974) measured the mean flow two up to two chords downstream of a NACA 0015 with a square tip using a two-dimensional laser velocimeter. He studied the flow for a variety of angle of attack and freestream velocities. He found that the axial velocity varied from a defect value of 0.88 to excess values of 1.05 and 1.18 for the higher angles of attack  $\alpha = 8, 10, 120$ , respectively.

In 1983, **Thompson**, using dye and hydrogen bubble flow visualization techniques studied the effects of various tip shapes on the vortex formation on a rectangular NACA0012 wing. the experiment was done in a water tunnel. The studies were performed using round, square and bevelled tip shapes at  $Re_c = 2.2 \times 10^4$  at various angles of attack. For the square and bevelled tip shapes, the separation was fixed by the sharp-edged boundary. For the rounded tip, the primary vortex was located on the rear portion of the suction side of the wing.

The work done by **Higuchi, Quadrell and Farell** (1986) and **Ikohagi, Higuchi and Arndt** (1986) showed that the available analytical models cannot accurately predict the near-field roll-up process, especially for cavitation prediction. Using LDV measurement to measure the mean flow up to 3.9 chords downstream of an elliptic wing, they show that the vortex cross-section was far from circular. They also found that the vortex core size was highly dependent on the angle of attack but previous analytical studies had found no such dependence.

Francis & Katz (1988) used a dye/laser sheet combination in a towing tank experiment to visualize the formation of a tip vortex on a rectangular NACA-66 hydrofoil. They tracked the location of the vortex core along the chordline and then developed empirical formulas for  $Rec$  ranging from  $1 \times 10^5$  to  $5 \times 10^6$  and for  $\alpha$  between  $0^\circ$ - $120^\circ$ . The formulas predicted that the vortex will increase in core diameter with increasing distance downstream while the path of the vortex centerline was found to move up and inboard. The opposite trends were predicted when the Reynolds number was increased. When the angle of attack was increased, the core diameter was found to decrease while the vortex moved up and inboard. Note however, that the empirical formulas were for a square tipped wing and may be less accurate when applied to the wing shapes.

Another study using different wing tip shapes was done by McAlister & Takahashi (1991) using two-component LDV to measure the mean flow behind a NACA 0015 wing. They used a square tip and a rounded tip at various conditions (chord size, chord Reynolds number, circulation, and downstream distance). For an angle of attack of 12 degrees, a maximum core axial velocity of  $1.5U_{inf}$  was measured at  $x/c=0.1$ . The trends in the flow structure was tracked by varying a single parameter while all the other parameters were held constant. In their study, they found that increasing the chord size (or circulation level) increased the tangential and axial velocities. However, increasing the Reynolds number decreased the tangential and axial velocities. Also, the rounded tip showed smoother separation characteristics and greater velocities than the square tipped wing.

### **3.3.0 Near- and Intermediate-Wake Flowfields (with Turbulence Measurements)**

An experiment by Poppleton (1971) was performed by injecting air into the core of a trailing vortex. The jet/vortex system was generated by airfoils set at equal and opposite angle of attack separated by a jet-pipe. Pitot probes, normal wires, and inclined wires were used to measure far downstream of the vortex. As to be expected, the jet increased the levels of turbulence in the core and the rate of decay of the vortex was increased also.

Chigier & Corsiglia (1971, 1972) used triple wires measurement techniques to measure up to 9 chords downstream of a square-tipped rectangular wing with NACA 0015 section. Within this measured flowfield, and for 12 degrees angle of attack and  $Rec=9.5 \times 10^5$ , they showed that the core axial velocity measured as high as  $1.4U_{inf}$  at  $x/c=-0.25$ , to a decay of  $1.1U_{inf}$ , and then accelerate slightly to a value of  $1.2U_{inf}$  at  $x/c = 4.0$ . At  $x/c = -0.5$ , the maximum crossflow velocity was measured to be  $0.42U_{inf}$  and it decayed axially afterwards. The decay in the crossflow velocity with axial direction should produce an adverse axial pressure gradient near the axis. Instead, their measurement showed an acceleration of the fluid on the core centerline. They found that the turbulence fluctuations were highest in the core and that the maximum turbulence intensity increase linearly with angle of attack. Similar to Thompson's study for a rectangular wing tip, they found a secondary vortex.

In 1973, Corsiglia, Schwind, and Chigier repeated the previous experiment using a rotat-

ing triple-wire traverse to eliminated the effects of meandering. Wind tunnel measurements are usually complicated by low-frequency unsteadiness (vortex meandering). The low-frequency unsteadiness will make any time-averaged Eulerian point measurement a weighted average in both space and time. (Meander can also be misinterpreted as turbulence). At  $x/c=26.7$ , the maximum tangential velocity was measured to be  $0.72U_{inf}$ . This was most 75% larger than the maximum tangential velocity measured using their old technique at  $x/c=-0.50$ . They attributed most of the discrepancy to the effects of meandering.

Mehta & Cantwell (1988) measured two of the three Reynolds shear stresses in a turbulent vortex generated by a half-delta wing., at relatively low Reynolds number. Distributions of Reynolds shear stresses were found to be consistent with the isotropic eddy viscosity concept.

Bandyopadhyay, Stead & Ash (1991) investigated the turbulence structure in a turbulent trailing vortex. They used a seven-hole pressure probe and single wires to measure up to 40 chordlengths downstream of the trailing edge at various freestream turbulence levels. In their study, they concluded that for their range of test conditions, the Rossby number was the controlling parameter for the turbulence structure, not the vortex Reynolds number. A lower Rossby number was found to promote re-laminarization. They also concluded that the inner core is not, as suggested previously, a region in nearly solid-body rotation that does not interact significantly with the outer region, but a re-laminarizing region where patches of turbulent fluid are intermittently brought in from the outer region.

Green & Acosta (1991) measured the instantaneous flowfield for up to 10 chords downstream of a rounded tip rectangular wing with NACA 66-209 section. At  $x/c=2$  and angle of attack of 10 degrees, the core axial velocity was measured to be  $1.6U_{inf}$ . Contrary to what other found the vortex he measured was axisymmetric at  $x/c=2$ .

Cutler & Bradshaw (1993) used cross-wires and pressure probes to study the interaction of a longitudinal vortex pair, generated by a delta wing, with a turbulent flat plate boundary layer. They observed that the lateral convergence of the boundary layer produced a drop in eddy viscosity, dissipation length scale, and skin-friction coefficient. They also found high levels of turbulence in the vortex core. Also, they found that the contours of the Reynolds shear stress were not consistent with well-behaved eddy viscosity.

Singh (1974), measured the mean and turbulent flow quantities for up to 85 chords downstream of a square-tipped rectangular wing with NACA 64<sub>3</sub>-618 section. He used quad-wires and single-wires for his measurements. A large axial velocity excess was found immediately downstream of the trailing edge for wings with large L/D ratios ( $>40$ ), while for lower L/D ratios, the vortex had a small axial velocity defect. The high L/D ratio wing measured a peak axial velocity of  $1.6U_{inf}$  at  $x/c=0.8$ ., but quickly decelerated to freestream level at  $x/c=2.4$  and then to an extreme velocity defect of  $0.52U_{inf}$  at  $x/c=5.0$ . The "instabilities" which developed downstream were analyzed by studying the axial velocity fluctuations and correlations.

### **3.4.0 Far-Wake**

Phillips & Graham (1984) used single normal and inclined hot-wired rotated to several orientations to measure the full Reynolds stress tensor in the far-wake of a vortex generated by a differential airfoil with trip for  $Re_c=7.4 \times 10^4$ ,  $\alpha = 90^\circ$ ). Three crossflow planes were studied, at 45, 78 and 109 chords downstream of the wing. The effect on turbulence of an axial velocity excess/deficit in the vortex core was simulated by placing a round jet or wake-enhancing nacelle in the center of the vortex generator. The profiles of the Reynolds stresses are close to what might be expected from mean flow considerations. They found that the jet had much faster turbulent decay than the wake, and this was attributed to the effect of the radial velocity. The jet had positive radial velocity which means that the vortex core was being compressed axially and widened, which they claim suppresses the turbulence.

The growth characteristics of trailing vortex wakes were investigated in the towing tank by Jacob, Savas and Liepmann (1996). The wake from a lifting wing rectangular NACA0012 airfoil with an aspect ratio of 8 were studied for up to 1400 chords downstream. The wake is mapped using digital particle image velocimetry (DPIV). The chord Reynolds number ranged from  $2 \times 10^4$  to  $6 \times 10^4$ . They chose this measurement technique since it gives continuous instantaneous planar velocity fields and is capable of eliminating problems associated with vortex wandering when mapping the flowfield with a single point probe such as a laser Doppler velocimeter or a hot-wire anemometer. They found that for these moderate Reynolds numbers at this high aspect ratio, the vortices are very stable and show little growth within the range of the measurements. This is reminiscent of viscous growth. The influence of the vortices upon each other is minimal. Also, they observed no Crow instabilities in these experiments.

## **4.0.0 COMPUTATIONAL STUDIES**

Most of the computational studies done on tip vortex flows focus on the roll-up of a vortex generated by a delta wing and of vortex breakdown. Few Navier-Stokes computations of the vortex roll-up process of a conventional wing exists. However, the tip vortex formed by a sharp geometry varies from that of a conventional wing like a rounded tip wing.

### **4.1.0 Formation and Roll-Up Process/Near-Wake (With Turbulence)**

A preliminary study by Mansour (1985) was one of the first attempts at using an implicit, three-dimensional thin layer Navier-Stokes solver to compute the flow around a transonic swept wing. His calculations indicated that the flow around the wing leading edge has a significant impact on the tip-vortex formation for this swept wing. However, his calculations predicted the leading-edge suction peak, shock location, and shock strength to be different from that measured by Keener.

Srinivasan et al (1988), studied the flow on a helicopter wing using ARC3d, a thin-layer Navier-Stokes solver using a zero-equation Baldwin-Lomax turbulence model. He

showed good qualitative agreement with the experimental work done by Spivey (197), but the resolution of the viscous wake and the surface pressure suction peak induced by the vortex was found to be poor.

In another computation by De Jong, Govindan, Levy, and Shamroth (1988), they used a forward-marching solver with eddy viscosity turbulence model to compute the flow around a NACA 0012 wing with a rounded tip. They used 225,000 grid points at a  $Re_c$  of  $7.4 \times 10^5$  and angles of attack of  $6.18^\circ$  and  $11.40^\circ$ . The location of the vortex core was accurately depicted but the key features were not predicted well, like the development of the axial velocity excess.

The computational study by Dacles-Mariani et al (1993, 1993) done in conjunction with the experiment by Chow et al (1991) studied the roll-up process for a NACA0012 rectangular wing at angle of attack of 10 degrees and  $Re_c = 4.6 \times 10^6$ . In this study the measured inflow conditions were used. Also, the wind tunnel walls were included in the computation. The solver used INS3D-UP which is based on the artificial compressibility method. The grid used was 2.5 million grid points with a modified BB model and SA model. They predicted an excess of axial velocity and compared well with experiment.

#### **4.2.0 Near-Wake/Turbulence/Engine Exhaust Interaction**

To date, the computation of the near-wake and the effect of engine exhaust on the vortex has not been fully studied. In a recent survey paper, Hoeijmakers (1996) recognized that the vortex wake/exhaust interaction is very complex and that the detailed modeling of this phenomenon has not been achieved. In the near-wake, the exhaust plume interacts with the development of the vortex. In the intermediate- and far-wake region, the exhaust gets trapped in the vortex. Generally, it has been assumed that the exhaust is trapped in the vortices but not all of it is entrained in the vortex core. This portion which is not trapped remains at the initial flight level and diffuses slowly in a relatively quiet air. The contrails which are captured by the vortices at first remain highly concentrated without too much mixing with the atmosphere. However, when the vortices are disrupted and they burst, they are suddenly released and dissolved.

#### **4.3.0 Intermediate and Far Wake**

Computational effort to simulate the intermediate and far-wake has been challenging. Since vortex wakes can persist for miles behind an aircraft, constructing a grid large enough with some degree of accuracy to resolve the wake vortex in this region has not been attained. Current computations truncate the domain close to the near-wake. Others model the wake when it comes to this region since the wake is pretty much inviscid and doesn't change much in structure.

## **5.0.0 WAKE VORTEX CONTROL AND MANAGEMENT**

In the early 1970's, a NASA wake-vortex program was started with the objective of alleviating or minimizing the vortex wakes shed by subsonic transport aircraft. Since that time, there has been a wide variety of ideas that were tried. Several will deintensify a vortex wake shed by the landing configuration of most subsonic transports, but despite all this, no practical and efficient means of accelerating the decay or managing the wake vortex has yet been found. This leaves the flight operations to coexist with the intense vortex wakes in the best way possible.

Currently (1997), NASA is revisiting this problem by addressing airport capacity enhancements through the terminal area productivity (TAP) program. The major goal of the TAP program is to develop the technology, during instrument meteorological conditions, which allows air traffic levels to approach or equal levels currently achievable only during visual operations. (Ref). A degradation in weather conditions causes a loss of visual approach capability. Some factors that make this possible include reducing the number of available runways and also influencing the longitudinal wake vortex separation constraints used by air traffic control (ATC) to space the aircraft in the runways.

The Aircraft Vortex Spacing System (AVOSS) Program, is currently being developed at NASA Langley as a subelement of the Reduced Spacing Operations (RSO) within the TAP program. AVOSS's primary goal is to integrate the output of several inter-related areas to produce weather dependent, dynamics wake vortex spacing criteria. These include current and predicted weather predictions, models of wake vortex transport and decay under these weather conditions, real-time feedback of wake vortex behavior from sensors, and operationally acceptable aircraft/wake interaction criteria. By considering ambient weather effects on wake transport and decay, the wake separation distances can be decreased during appropriate periods of aircraft operation.

The vortex pair produced by the lifting surface of the aircraft induces lifting, yawing and pitching motions on the following aircraft. However, the rolling moment that the vortex pair induces is the most hazardous feature of the wake. For this reason, research on the characteristics of the vortex wakes produced by aircrafts has concentrated on the structure of these wakes and the rolling moment that they induce on the following aircraft. Typically, the strength of vortex wakes decays over some distance in the wake but there is some amplification that may also occur because of the vortices taking a sinuous shape caused by atmospheric (or wind-tunnel) turbulence (Rossow et al 1996).

### **5.1.0 Experimental Studies**

Mason and Marchman (1973) studied the far-field structure of aircraft wake turbulence at stations up to 30 chords downstream of a rectangular wing. They obtained detailed flow measurements and showed that mass injection at the wingtip accelerated the vortex decay process.

### 5.2.0 Computational Studies

Wong & Kandil (1992) studied the effects of angled wing-tip blowing on the behavior of trailing vortices. They computed the flow-field of a large aspect-ratio rectangular wing using the thin-layer Navier-Stokes equations using a NACA0012 wing and a rounded tip configuration.

### 6.0.0 Wake Modeling

**Lanchester** (1907) pioneered the concept of the trailing vortex generated from a lifting surface. He argued that the bound vorticity associated with the wing's lift could not stop at the wingtip; this would be in violation of Helmholtz's theorem which states that a vortex cannot begin or end in the flow. Further he hypothesized that the work needed to produce lift in this flowfield is associated with the kinetic energy which in turn is related to induced drag; where it is defined as the kinetic energy added to the wake per unit distance traveled by the wing of finite span.

**Prandtl** was the first to put Lanchester's concept into a complete mathematical model universally known as "Prandtl's lifting line theory". Here, he represents a finite wing as a concentrated lifting "bound" vortex, with trailing wake vortices extending to infinity in the downstream direction. In Prandtl's inviscid potential model, the vortex wake extends to infinity. However, in a real viscous flow, the vortex wake eventually breaks down and the kinetic energy transferred to heat through viscous dissipation. But this takes place far downstream that the infinite-wake model is still useful. The generalization of the lifting line model to nonplanar lifting system was studied by **Cone**<sup>2</sup> where he found optimal load distributions for a variety of shapes, including elliptical 'spanwise camber', simple dihedral, winglets and fully closed ring-wings. All these analyses relied on the circulation being concentrated on the "lifting line". Based on **Munk's** stagger theorem, this model should be adequate for studies of induced drag. But the issue of how to build a real wing to produce the desired loading, was not addressed. An obvious difficulty is that the downwash on the actual surface varies somewhat from the value computed on the lifting line. This influence is most dramatic near the wingtip, where the three-dimensional flow makes the load distribution depart from that predicted by **Glauert's** method. Later work by **Weissinger** and others addressed the problem of loading on a general lifting surface by numerically solving a collocation problem that represents the kinematic boundary conditions on the mean surface of the wing. This approach has evolved into the discrete vortex-lattice and high-order panel methods.

The classical wing theory described up to this point requires that the wake shape be prescribed. The streamwise wake model consisting of straight vortex filaments leaving the trailing edge in the freestream direction is the most widely used. Prandtl's justification for this model was that although the true force-free wake may be considerably deformed in the far-field, this "roll-up" occurs slowly so that the near-field portions of the wake, which

have the most dominant influence, are not significantly altered from their initial shape.

### 6.1.0 Modeling Techniques

**Von Karman** developed the far-field approach for determining induced drag from properties in a transverse plane far downstream of the wing (Ref). This procedure has become known as “Trefftz plane” drag integration, since **Trefftz** employed the far-field plane in connection with a slightly different problem. With the development of this far-field drag computation technique, there was heightened interest in attempting to model the force-free wake shape. **Betz** developed a variety of theorems concerning the motions of systems of infinite vortices. The basic idea of the Betz method is to replace the difficult computation of the precise details of the inviscid roll-up of the vortex sheet with a local axisymmetric distribution of vorticity. **Spreiter** applied Betz’s rules, with some 3-d considerations to allow an approximation of the three-dimensional rolled-up wake trailing from finite wings. Since then, a variety of computational techniques have been employed for iteratively relaxing the trailing wake to the force-free shape. Representative examples are the unsteady vortex-lattice method of **Mittleman**(Ref), and **Quakenbush**(Ref).

Discrete vortex wake models require a viscous-core model to modify the velocities induced very close to the vortex singularity. Lamb’s core model is widely used to prevent erratic behavior of the vortex filaments as they pass near each other. An analogy to the viscous core model applied to distributed vorticity wake model is described by **Ramachandran** applied to the finite-difference solution of the full potential equation. Finally, the vortex-in-cell methods of **Ribeiro** is a recent method to relax the wake shape. More recent studies of induced drag characteristics of finite wings have been done using the modern lifting surface computational methods.

By correlating with experimental data, **McCormick et al** [1968], **Roberts** [1975,1984], **Phillips** [1981] proposed analytical scaling laws to describe the structure of viscous turbulent trailing vortices with some success. Various experimental studies involving scaled model testing using wind-tunnels and full-scale flight testing were also carried out especially in the 1970s (**Olsen et al** [1971], and **Hallock** and **Eberle** [1977]).

Current wake models which address the intermediate-wake region are basically first-order methods and do not necessarily include the viscous upstream effects and the turbulence structure. They are mostly inviscid models which do not account for the diffusion and aging process of the wake. To date, there are two ways of modeling the inviscid wake vortex flow. The first class of methods uses an Eulerian approach. These methods have fixed reference frames and solve the governing equations for continuity and momentum, (and energy for compressible flows) in the absence of viscosity. They do not require specify the shape of the vortices. One shortcoming of this method is the presence of numerical diffusion which overwhelms the physical diffusion. The resulting effect is that the vortex diffuses to a much larger size, unless a large number of grid points is used. On the other hand, using a large number of grid points excludes the capability of the wake model for practical purposes. A model proposed by **Steinhoff et al** (19 ) solves the Navier-Stokes equations which has been modified to include a ‘vorticity confinement’



term in the momentum equations. The effect of the term is to confine the concentrated vorticity to thin regions which extend over a few number of grid points. However, the internal feature of the wake vortex is not resolved and the viscous upstream effects has been completely neglected.

The second class of methods solves the inviscid wake vortex problem using Lagrangian markers which are allowed to convect with the flow. These methods are the 'Vortex Lattice' or 'Vortex Blob' methods for incompressible flow applications, or 'Vortex Embedding' methods for compressible flow applications. Essentially, these methods represent the vortex sheets (or filaments) using surfaces (lines) defined by markers. The main interest in these models are the total vorticity around each point of a centroid and its location. To account for the physical diffusion, a 'spreading' function is specified which effectively defines the internal structure of the vortex. Since this structure is specified, it can be kept constant or varied slowly to simulate physical diffusion. Although it avoids the numerical diffusion of the Eulerian methods, the prescription of the 'physical diffusion' is still empirical. The topology of each of the vortical regions should be known beforehand so that a suitable array of markers can be computationally defined. In some instances, this may not be a realistic assumption as when more than one vortex sheet is shed from different places with some possibility of reattachment. This makes the marker specification difficult to accomplish. For some applications, the Vortex-Lattice Method is suitable because of its ease in application to a large variety of aircraft configuration. Also, the required computing time to complete one calculation is not computationally intensive. However, the issue of accuracy is still problem and flow depended. Rossow, validated the Vortex Lattice Method for computing the loads induced on aircrafts they encounter lift-generating wakes. His study concluded that for small following wings, the Vortex Lattice Method was reliable in computing the lift and rolling-moment distribution. However, as the span and planform area of the encountering wing become larger, the method became less accurate.

## **6.2.0 Wake Vortex and Ground Interaction**

For sufficiently large Reynolds Number, when a vortex ring approaches a solid surface at normal incidence, the unsteady adverse pressure gradient on the wall results in the separation of the boundary layer. As a result, a secondary vortex ring is formed which has an opposite sign. Studies by Walker(Ref), Doligalski and Walker () suggest that the boundary layer induced by a vortex ring will always separate, but the intensity of the resultant inviscid/viscous interaction will be governed by the strength of the primary vortex had how closely it approaches the wall. Many studies have observed that the core of the primary vortex ring moves downward and outward along the path predicted by the inviscid theory, until an eruption of boundary layer fluid occurs. This causes a reversal of the primary core's parth and is known as vortex 'rebound'.

Cerra and Smith () and Walker, et al. performed an extensive account on the position and interactions of different regions of vorticity using flow visualization. They noted that for higher Reynolds numbers both secondary and tertiary vortex rings form, and the secondary ring is ejected away from the wall. A study by Fabris, using Digital Particle Image

Velocimetry (DPIV) is applied to the ring/wall flowfield for a wide range of Reynolds numbers. The creation of the secondary and tertiary vortex rings were observed, but not the ejection of the secondary ring. The main point of their study is that the tertiary ring formed due to a Kelvin-Helmholtz shear layer instability, and that the unsteadiness of the secondary ring initiates a three-dimensional breakdown of the flowfield which inhibits the ejection of the secondary ring.

Gendrich, Bohl, and Koochesfahani (1997) performed a whole-field measurement of unsteady separation in a vortex ring/ wall interaction using a 2-color Laser-Induced Fluorescence (LIF) and Molecular Tagging Velocimetry (MTV). They experimentally studied the process of boundary layer separation, the formation of the secondary vortex ring and its ejection from the wall. Their work provided a detailed measurement of the vorticity field. The results based on the MTV data and the two-color laser-induced fluorescence (LIF) visualizations indicated that the pairing of the secondary and tertiary vortex rings is not an essential physical mechanism leading to the ejection of the secondary vortex ring from the near-wall region.

### **6.3.0 Wake Vortex with Atmospheric Modeling**

Improving the efficiency and accuracy of forecasting system for air safety require some understanding of the dynamics of aircraft induced wake vortices within the atmospheric boundary layer. Observations and measurements of moving wake vortices show large variations with respect to atmospheric boundary layer (ABL) conditions, such as the background wind, wind shear and stratification (Burnham). For example, the vortex lifetime appears to be limited mainly by ambient turbulence effects in the planetary boundary layer(ref). To date, there is very little significant work done on this.

Trailing vortices generated by a lifting surface moving through air leave behind a complex environment. The atmosphere is stratified vertically since its density, temperature and pressure all vary with altitude.

Recently, there has been a number of experimental studies done on the behavior of wake vortices in stratified and unstratified water (Sarpkaya, 1983). The experiments were conducted with three delta wings and two rectangular wings. The evolution of the trailing vortices were investigated and the vortex trajectories determined. He showed that the vortices rise only to a finite height and then decay gradually at first and then rapidly thereafter under the influence of turbulence, sinusoidal instability and core bursting. The effect of stratification is also to reduce the lifespan of vortices and the maximum height they attain.

A simple empirical model for the transport and decay of aircraft trailing wake vortices has been studied by Kantha (1996). Here the vortices between parallel runways in a turbulent atmosphere has been considered. The model includes the influence of ambient turbulence on the decay rate of the vortices as well as the effect of the crosswind shear. In

this study, he found that ambient shear plays an important role in vortex decay and transport. He also found that atmospheric stability also affects the fate of these vortices. However, stable stratification has a much larger effect than convective heating of the atmospheric boundary layer.

Corjon, et al (1997) performed a three-dimensional direct numerical simulation of a vortex pair, placed in a laminar flow near the ground which is representative of a neutral surface boundary layer. The effect of variable crosswind shear on the rebound is studied with the effect of an axial wind. They show that long wavelength variation of the crosswind induces a curvature of the secondary vortices. They also found that this curvature is self amplified and leads to their reconnection with the primary vortices. The linking was found to make the vortex collapse.

#### **6.4.0 Wake Vortex Pair Interaction**

Jacob, et al (1997) studied the fundamental physics of vortex interaction, such as that encountered among the wingtip and flap vortices in the wake of an aircraft. A traversing five-hole pitot probe and Lagrangian Parcel Tracking (LPT) are used to measure the velocity field in a cross-stream plane behind the wing. The measurements were performed both in a towing tank and wind tunnel. The wind tunnel measured 0.81 m x 0.81 m and is 3.7 m long. The wind tunnel test facility was chosen since it allows detailed time-averaged measurements of the near-wake in a plane flowfield relative to the wing. The towing tank is approximately 70 m long and 2.4 m across with a nominal depth of 1.5 m. The towing tank allows measurement of the entire evolving wake in a plane fixed relative to an observer. The study also included some 'realistic effects' such as adding engines with and without thrust or fuselage wake effects and how it affects the vortex interaction. They found that at low Reynolds numbers, the vortex decay before they have a chance to interact. At high Reynolds numbers, the vortices merge before diffusion significantly alters them. The merging of the flap and the tip vortices usually occurs within one orbit, leading to a shorter descent distance.

Devenport, et al (1997) performed experimental studies on the structure and development of a counter-rotating wing-tip vortex pair. The vortices were generated by two rectangular NACA 0012 half wings placed tip to tip, and separated by 0.25 chordlengths. From their preliminary studies, they found that the vortices were insensitive to the introduction of a probe and subject only to small wandering motions. They made three-component velocity measurements at 10 and 30 chordlengths downstream of the wing leading edges for  $Re = 2.6 \times 10^5$ . They found that at 10 chordlengths downstream, the vortex cores are laminar. The turbulence levels within the cores are low and vary very little with radius. The turbulence that surrounds the cores is formed by the roll-up of and the interaction of the wing wakes that spiral around them. At 30 chordlengths, the vortex cores were found to have become turbulent. The turbulence levels within the vortices are larger and increase rapidly with radius. The turbulent region surrounding the cores has doubled in size and turbulence levels have not diminished. The distribution of the turbu-

lence has also been changed. Now, the wake spirals have been replaced by a much more core-centered turbulence field. They also point out that the flow structure they obtained for the vortex pair flow sharply contrasts with what has been seen in the equivalent isolated tip vortex. Here, the vortex core remains laminar and the turbulence surrounding it decays rapidly with downstream distance. This implies that the transition to turbulence in the cores of the vortex pair is stimulated by interaction between the vortices. Spectral measurements at 10 chordlengths suggest that short-wave instability may be the cause.

### **7.0.0 High Lift Systems**

The flow over high lift configurations is quite complex. Multi-element flows contain areas of laminar separation, transition, strong adverse pressure gradients and turbulent separation just to name a few.

#### **7.1.0 Experimental Studies**

Storms, Takahashi, and Ross (1996), studied the aerodynamics of a simple three-dimensional high lift system. The effects of the part-span flap and slat on the tip flow fields are measured in detail. One of the objectives of the experiment is to provide a database for CFD validation by performing wake surveys one chord from flat trailing edge. What they found was that relative to a two-dimensional high lift system, the part-span flap introduces a spanwise lift. Multiple vortices at the flap tip were also found. For the part-span slat, they found that this configuration exhibits an early stall relative to the full span for slat and that there was a single vortex at the slat tip.

#### **7.2.0 Computational Studies**

Rogers (1993) presented some calculations on high lift aerodynamics calculations in either a take-off or a landing configuration. The computational approach utilizes an incompressible Navier-Stokes flow solver (INS3D-UP) and an overlaid chimera grid approach. He performed some detailed grid resolution study for flow over a three-element airfoil using a one-equation Baldwin-Barth turbulence model and a two-equation  $k-\omega$  model. He found good agreement with experiment for the lift coefficient at all angles of attack. Some three-dimensional results are presented for a wing with a square wing tip.

A computational study of a semi-span flap in a three-dimensional configuration was performed by Mathias et al (1997). They investigated one of the principles of a three-dimensional feature of the flow over a high-lift system, which is the flow associated with the flap edge. Flow computed over a two-element high lift configuration using INS3D-UP with structured overset grid and one-equation Baldwin-Barth mode was performed. The geometry was based on a NACA 63<sub>2</sub>-215 Mod. B airfoil section (Ref) configured with a 30% chord Fowler flap and 30 degree flap deflection. The analysis was done for Reynolds number (based on unflapped airfoil chord) of  $3.7 \times 10^6$  and angle of attack = 10

degrees. Comparisons showed good agreement with the experiment.

## **8.0.0 ISSUES IN NUMERICAL STUDIES**

### **8.1.0 Spatial Order of Differencing Scheme**

Difficulties encountered in tip vortex flow simulation can be attributed to some numerical issues such as the spatial order of accuracy.

Rai (1987) studied the numerical simulation of blade-vortex interaction using higher-order accurate upwind schemes. He concluded that conventional, spatially second-order-accurate, finite-differencing schemes are much too dissipative for calculations involving vortices that travel large distances. A fifth-order accurate, upwind-biased scheme was found to preserve the vortex structure for much longer times than existing second-order accurate, central and upwind differencing schemes.

The effects of spatial order of accuracy in computing vortical flowfields was analyzed by Ekaterinaris (ref 1991), for the resolution of the leading-edge vortices over sharp-edged delta wings. The flowfield is computed using a viscous/inviscid zonal approach. High-order, upwind-biased, finite-difference formulas are used to evaluate the derivative of the nonlinear convective terms. The computed results show that a higher-order of accuracy enables better convection of the vorticity (i.e. less diffusion) and produces close agreement with measured surface pressures.

Dacles-Mariani et al (1994), studied the effect of fifth-order vs. third-order upwind-biased flux differencing scheme using the INS3D-UP solver. They found that the third-order differencing technique is still very dissipative for flows with high gradients such as vortical flows. The accuracy was improved when the fifth-order differencing technique was used.

More recently, Wake, et al (1996), investigated the effects of high-order upwind differencing for vortex convection. He tested an inviscid Lamb vortex and found that the 5th-order scheme provided a factor of 10 reduction in the number of points over the 3rd-order scheme in each crossflow plane. What they found was that although the higher-order schemes improved the results, it was found that the axial grid spacing was limited.

### **8.2.0 Transition/Turbulence Modeling**

Dacles-Mariani et al (1993) found that turbulence modeling also contributes to the dissipation of the vortex core. They found that existing one-equation turbulence models such as the one-equation Baldwin Barth turbulence model and the Spalart-Allmaras turbulence models are too dissipative to be applied to vortex flows. A modification of the production term of the turbulence has to be implemented in order to reduce the dissipation in the viscous vortex core. Note however, that the modification does not affect the boundary layer but only depresses the turbulence level at the viscous vortex core.

The work by Zeman (1994) employed a full Reynolds stress model to study the far-field nature of the turbulence in an isolated vortex. He predicted a rapid decay of the initial turbulence in the vortex core.

Turbulence modeling in the wake region can be classified into two classes. The first class of modeling is a two-dimensional study of wake vortices with the turbulence modeled explicitly or parametrized. They were mostly used to study wake vortices in free atmosphere as well as their interaction with the ground. (Bilanin et al (1977), Robins et al, 1988). The second classes is the three-dimensional model of infinite-length vortices which use idealized initial and boundary conditions. They used either periodic or other simplified conditions and no background turbulence or stratification is accounted for.

Spalart and Wray studied the behavior of periodic vortex lines embedded in homogeneous isotropic turbulence. They found a relatively large spread in the destruction time for the wake vortices.

Gers et al (1996) found that small scales of turbulence served only to cause small distortion in the vortices, while larger scales cause the large deformation which lead to Crow instability.

The study by Schowalter et al (1997), presented a large eddy simulation method of the aircraft wake vortices embedded in planetary turbulence. They described the nested grid technique and wake vortex boundary initial conditions for large-eddy simulation.

### **8.3.0 Outflow Boundary Condition**

One of the shortcomings of vortex flows is that these vortices persist for miles downstream of the trailing edge. Typical calculations truncate the flowfield to a shorted distance but this requires that the outflow boundary condition is known. Others stretch the grid such that the wake is geometrically expanded in the streamwise direction and then prescribe uniform pressure at the outflow. The problem with this is that this prescription is very empirical. Some of the physical features of the flow can also be lost.

### **8.4.0 Adaptive Gridding**

In the near-field region where tip vortex flows is highly complex, with existence of large flow gradients, the number of grid points required can be quite large. Adaptive gridding is therefore needed to reduce the total number of grid points. In the intermediate-wake region, since trailing vortices do not decay right away, adaptive gridding to follow the essential feature of the wake vortex is needed in order to maintain accuracy.

## **9.0.0 INSTABILITIES**

Some of the well known decay mechanisms for wake vortices are the Crow instability and vortex breakdown. The Crow instability results in vortex lines forming vortex rings while vortex breakdown or 'bursting' is associated with rapid core expansion due to large variation in axial velocity. The Crow instability is an exponential growth resulting in either linking of the vortex pair into a series of crude vortex rings or in a highly disorganized intermingling of the vortices. Vortex breakdown, rearranges the vortex structure and increases the core size, turbulence and energy dissipation. Because of these, it is often very difficult to accurately measure the trajectories of the three-dimensional vortices.

Some recent stability studies delineate the effects due to short and long wavelength instabilities (Klein et al 1995). They find that the Crow theory is an application case of a more general theory. They show that a vortex pair is always unstable when its circulation ratio is negative. In another study, Marshall et al showed three different types of instability of a vortex pair immersed in a cross stream shear flow for long-wave perturbations: mutual interaction of the two vortices of the pair (which is symmetric), interaction with the vortex that has vorticity of the same sign and antisymmetric waves.

### **9.1.0 Crow Instability and Small Scale Instabilities**

For a given pair of counter-rotating vortices generated from a lifting wing, these vortices descend, for an unstratified fluid, and evolve into a series of vortex rings via a sinusoidal instability. This was first reported by Scorer (1955), and was analyzed first by Crow (1970) in an unstratified fluid. Crow's instability results in vortex lines forming vortex rings. His predictions have been verified in the laboratory (Sarpkaya,) and studied computationally by Robins and Delisi (1997)

The vortex evolution is different, however, for stratified flows. It was found in 3D laboratory experiments that stratification inhibits the vertical migration of the vortices (Sarpkaya), which was also observed in 3D numerical simulations (Robins and Delisi). Spalart (1996), performed a high resolution, 2D study reporting that the distance between the vortex cores became smaller in a stratified fluid, and the vortices propagated farther in a nonstratified fluid.

In the experiments reported above, none of them reported on small-scale instabilities in the flow. However, Devenport et al (1997) reported on laboratory experiments where small-scale structures were observed ten chords behind the wings (the experiments were measured near the trailing edge of two half-wings). Also, Delisi et al (1997) examined the three-dimensional behavior of wake vortices in density stratified fluids and have observed instabilities much smaller than the Crow instabilities. However, at this moment, a comprehensive theory as to why these small scales are observed at later times in a stratified flow and appear to be absent in a nonstratified flow is lacking.

### **9.2.0 Vortex Burst/Breakdown**

At high angles of attack, vortices can experience a phenomenon called vortex burst/ breakdown. The vortex breakdown, or vortex burst is usually characterized by a sudden expansion in the vortex core and a change in the coherent structure of the vortex. In experiment, some researches categorizes the two types of breakdown as a bubble vortex breakdown (vortex burst) and a spiral vortex breakdown; although other researchers argue that this separation cannot be made. In both cases, the axial velocity component decelerates and stagnates on the vortex axis. For a vortex burst a zone of recirculating flow is seen in the vortex core where as in the spiral vortex breakdown this is not observed. In other words, flow changes in the vortex core from a jet-like to a wake-like flow for a vortex burst scenario.

The vortex burst phenomenon has been a subject of much study both experimentally and theoretically (Lambourne, 1961), and Escudier, (1988). Most of the theoretical studies performed so far have been on relatively simple cases such as a vortex confined in a tube or an isolated vortex. A lot of experiments have also been performed on the breakdown of both free and confined vortices, however, no general agreement regarding the essential nature of vortex breakdown exists.

Some visual techniques to determine vortex breakdown uses smoke particles and laser light sheets and Schlieren systems (Wentz et al 1968, O'Neil, et al, 1989, and Cornelius, 1990). The criteria each experimentalist select as the point of vortex breakdown differs because each has adopted different criteria to do so. Experimentally, One criteria used to determine vortex breakdown is by flow visualization. Upstream of the breakdown, the vortex core appears a smoke-free dark colored region at the center of the vortex. At the onset of vortex breakdown, the dark core region disappears as smoke enters this area for the first time. The disappearance of the smoke-free core region at the breakdown is due to flow stagnation at the core.

From a numerically determined solution, vortex breakdown is currently a post-processed issue. The onset of vortex breakdown has been based on the collapse of the rolled-up shear layer, and on the stagnation or asymmetry of axial velocity contours (O'Neill , 1989, and Agrawal, et al , 1990).

Robinson, et al (1991) introduced a simple criterion based on an integral formulation of the Rossby number to predict vortex breakdown. In their study, they reconnect that in the Rossby Number range of 0.9 to 1.4, values below this range indicate a burst vortex while values above this range indicate a stable vortex.

### **10.0.0 OTHER RELATED TOPICS**

Tip vortex flows are not only limited to aircraft configuration. Some of the other engineering problems where it is encountered is outlined next.

### **10.1.0 Rotorcraft Vortex Wakes**



McCroskey (1995) presented an overview of the wakes of rotary-wing aircraft. These wakes affect the performance, noise and vibration of the rotorcraft. In this review paper, he outlines some of the recent attempts to measure, predict and control these phenomena mentioned above.

Most of the aerodynamics problems found in rotorcraft flows arise from some aspect of the tangled vortex wake system from the main and tail rotor blades as they rotate and translate in flight. The shed vorticity from the rotor blades tends to initially roll-up into discrete, concentrated tip vortices that remain approximately in a cycloidal trace of the blade tips. The blade/vortex interaction (BVI) is one aspect of the rotorcraft flow wherein the wake vortex interact with the rotor blades. This important problem has received considerable attention.

In his paper, he discussed some of the experimental techniques currently being used for studying the wake structure of a helicopter in forward flight. He also reviewed some of the theoretical and numerical wake vortex methods. One particular subject of interest is the hybrid coupling of the vortex wakes with the CFD codes. Tung et al (1986), presented an iterative method where they coupled the CFD codes for the nonlinear near-field with various vortex methods for the wakes. A more detailed presentation of their work is given in Ref. (Tung 1986).

### **10.2.0 Tip Leakage Vortex**

The turbulent structure of a tip leakage vortex wake was studied by Devenport et al (1997). Here, they concentrated on investigating the flow downstream of a linear turbine cascade with tip gap using a three-component velocity measurements made using a miniature four sensor hot wire probes. They found that much of the turbulence appears to be generated by streamwise velocity gradients that surround the vortex core. But the most intense velocity fluctuations appears close to the wall in the region where the secondary flow of the vortex is lifting fluid away from the wall. Numerous studies of tip gap flow and formation of tip leakage vortices exist in literature. However, the main focus of their study was to gain detailed understanding of the turbulent structure of the tip leakage vortex wakes. Their data showed in detail the cross-section turbulent structure of the flow including blade wakes and tip leakages.

### **10.3.0 Ship Propeller Blade Cavitation**

Tip vortices are also present in ship propeller blade specifically with the cavitation of ship propeller blades due to the presence of the low pressure in the vortex core.

Arndt, et al (1994) recently studied the physics of cavitation inception in trailing vortices, where they verified that the cavitation inception occurs close to the tip. In their paper, they noted that 'progress in understanding the details of the inception process has been hampered by a lack of sufficient knowledge about the structure of the tip vortex very close to the tip'. In their study, both numerical and experimental studies were performed.

They studied cavitation inception using a series of elliptical planform hydrofoils with different cross section. They found that the boundary layer characteristics were different for each kind. However, the process of vortex roll-up appears to be similar. The numerical calculations using a large eddy simulation technique provided some qualitative information on the details of the vortex formation. One feature they noted is the interaction between the viscous wake and the tip vortex. Unfortunately, the numerical model was not able to accurately predict the minimum pressure in the vortex which they attribute to lack of sufficient spatial resolution. However, they were able to predict the minimum pressure location to be very close to the tip which qualitatively in agreement with the experiment.

Eca, et al (1994) investigated the tip vortices generated by marine propellers. In their study, he emphasized the fact that tip vortex cavitation is usually the first type of cavitation to appear on ship propeller blades. It can also be a major source of noise. Design optimization must require the accurate prediction of a propeller's behavior with regard to tip vortex cavitation, either by experiment or by computation. His work concentrated on a numerical effort to solve the incompressible viscous flow at the tip of wings with an elliptical planform. He showed some good agreement with the experiment as far as the vortex position and some general flow characteristics, but the vortex core size is over estimated.

Souders, et al (1981), experimentally studied the fundamental aspects of tip vortex cavitation characteristics and the delay of inception on a three-dimensional hydrofoil. The results for the tip vortex cavitation delay concepts indicate substantial increases in the tip vortex cavitation inception speed relative to an unaltered tip. The results were obtained over a wide range of foil angle of attack and showed little or no measurable loss in foil performance.

### **11.0.0 VISUALIZATION TOOLS FOR VORTICAL FLOWS**

In aerodynamics and fluid dynamics, flow visualization has played an important role in further understanding some complex physics in the flowfield wherein vortical flows are present. Most of the investigators use the concept of swirling flow as one means of locating vortices in a flowfield. Some of the algorithms that were developed to track vortices are by Moin and Kim (1985,1986), Villasenor and Vincent (1992), Globus et al (1991), Banks and Singer (1994), and Jeong and Hussain (1995).

In a recent work by Kenwright and Haines (1997), an eigenvector method used for vortex identification has been applied to recent numerical and experimental studies in aerodynamics. They show that their method can extract and visualize salient features of the flow such as vortex cores, spiral vortex breakdown, vortex bursting and vortex diffusion.

A specific application of this method is the numerical/experimental work of Dacles-Mariani, Zilliac, Chow and Bradshaw (1995). Some of the features that are needed for comparison between computed and measured results are the location of the vortex core and the trajectory of the vortex. Currently, one of the techniques used to locate the vortex core involves finding the minimum crossflow velocity within the vortex core region. This can

prove to be tasking for large data sets. Also, near the wing where the vortex is still forming, it is not easy to detect the core of the vortex. The method used by Kenwright et al was able to trace back the vortex core location to its origin in the boundary layer in an automated fashion.

## **12.0.0 FURTHER WORK NEEDED**

To date, there are still several obstacles to the development of a better understanding of the important features of trailing vortices (Sarpkaya, 1983). The first is the *roll-up process*. The flow distribution (velocity, turbulence, etc), at any station behind the wing depends on the wing section, wing tip shape, Reynolds number wing incidence and the distance of the station from the wing. A change in tip shape changes the core size, velocity and turbulence distribution. The high levels of turbulence result in an increased diffusion of vorticity which in turn increases the core size. *Probe sensitivity* of the vortices is another issue to be considered. Flow-visualization studies suggest that trailing vortices are extremely sensitive to disturbances created by very small probes. Non-intrusive type of measurements such as LDV has been used but even then, vortex wandering', (Baker et al 1974), which makes the vortices appear larger than normal in time-averaged velocity measurements (for vortices in wind tunnel setting), or the unsteady nature of the flow makes the velocity profiles difficult to determine. There is also present, some *large scale instabilities*. The vortices were never observed to decay away from viscous and turbulent dissipation, but were always destroyed by either mutual induction stability (Crow instability) and/or vortex breakdown. Next is the *Reynolds number*. The highest Reynolds numbers (based on wing chord), that is reached in wing tunnels or towing tanks are an order of magnitude lower than what is possible for an aircraft. Because of this, the scale effects are not easy to study. Finally, *ambient conditions*, such as background turbulence and atmosphere stratification play major roles in the evolution of the vortices.

In order to form a complete picture of the trailing vortex from its roll-up and formation on the wing to its far-field behavior, one aspect of the flow is lacking to be studied computationally. The near-field behavior of an aircraft with the effect of the engine exhaust, and turbulence on the vortex still needs to be simulated or modeled. Presented in the Appendix is an outline of the complete characterization of wake vortex flow from its formation on the wing to the wake region. In this section, it outlines previous and ongoing work on this subject and emphasized future areas for research.

## **13.0.0 ACKNOWLEDGEMENT**

The author would like to thank Drs. Dochan Kwak, Vernon Rossow, Jim McKroskey and Greg Zilliac for their helpful discussions on this research subject.

## **14.0.0 REFERENCES**

Coloni, T., Lele, S., and Moin, P., 'The free compressible viscous vortex', J. Fluid

Mechanics (1991), vol. 230, pp 45-73.

Mayer, E, and Powell, K., 'Similarity solutions for viscous vortex cores', J. Fluid Mechanics (1992), vol. 238, pp 487-507.

Spalart, P. 'Airplane Trailing Vortices', to appear in Annual Review of Physics. (1997).

Rossow, V., 'Wake-Vortex Structure from Lift and Torque Induced on a Following Wing', AIAA-93-30313, AIAA 24th Fluid Dynamics Conf, July 6-9, 1993, Orlando, FL.

Milne-Thompson, L.M., Theoretical Hydrodynamics, 8th ed., The MacMillan Co., New York, 1960, pp 353-4. (Rankine vortex)

Lamb, Sir Horace, Hydrodynamics, 6th ed., Dover, 1945, pp 591-2.

Rossow, V. J., 'Prediction of Span Loading from Measured Wake-Vortex Structure-An Inverse Betz Method', AIAA Journal of Aircraft, Vol. 12, No. 7, July 1975, pp 626-8.

Burgers, J.M., Advances in Applied Mechanics, 'A Mathematical Model Illustrating the Theory of Turbulence', Vol. 1, pp 197-199. Academic Press, 1948.

Rott, N., On the Viscous Core of a Line Vortex, ZAMP, Vol. 9b, No. 5/6 pp. 543-553, 1958.

Jacob, J, Savas, O., Liepmann, D., 'Trailing Vortex Wake Growth Characteristics of a High Aspect Ratio Rectangular Airfoil', AIAA Journal, Vol. 35, No. 2, Feb. 1997.

Perry, R.B., Hinton, D., and Stuver, R., NASA Wake Vortex Research for Aircraft Spacing, 35th Aerospace Sciences Meeting & Exhibit, Jan 6-10, 1997, Reno, NV. AIAA 97-0057.

Donaldson, C., Snedeker, R., and Sullivan, R., 'Calculation of Aircraft Wake Velocity Profiles and Comparison with Experimental Measurements', Journal of Aircraft, Sept. 1974. Tombach, I., 'Observations of Atmospheric Effects on Vortex Wake Behavior', Journal of Aircraft. Nov. 1973.

Lambourne, N.C. and Bryer, D.W. 'The Bursting of Leading-Edge Vortices' - Some Observations and Discussion of the Phenomenon', A.R.C., R. % M., No. 3282, April 1961.

Escudier, M., 'Vortex Breakdown: Observations and Explanations', Progress in Aerospace Sciences, Vol. 25, 1988, pp. 189-229.

Leibovich, S., 'Vortex Stability and Breakdown; Survey and Extension', AIAA Journal, Vol. 22, No. 9, Sept. 1984, pp. 1192-1206.

O'Neill, P.J., Barnett, R.M., and Louie, C.M., 'Numerical Solution of Leading-Edge Vortex

Breakdown Using an Euler Code', AIAA-89-2189, July 1989.

Agrawal, S., Barnett, R.M., and Robinson, B., 'Investigation of Vortex Breakdown on a Delta Wing using the Euler and Navier-Stokes Equations', AGARD-FDP Symposium on Vortex Flow Aerodynamics, Paper No. 24, October, 1990.

Ekaterinaris, J.A., and Schiff, L.B., 'Vortical Flows over Delta Wings and Numerical Prediction of Vortex Breakdown', AIAA-90-0102, Jan. 1990.

Robinson, B.A., Barnett, R.M., and Agrawal, S. 'A Simple Numerical Criteria for Vortex Breakdown', AIAA Paper, 1991.

Arndt, R., and Maines, B., 'Viscous Effects in Tip Vortex Cavitation and Nucleation', 20th Symposium on Naval Hydrodynamics, Santa Barbara, CA Aug. 1994.

McCroskey, W.J., 'Vortex Wakes of Rotorcraft', 33rd Aerospace Sciences Meeting and Exhibit, Jan 9-12, 1995, Reno, NV, AIAA95-0530.

Tung, C., Caradonna, F.X., and Johnson, W., 'The Prediction of Transonic Flows on Advancing Rotors', Journal of American Helicopter Society, Vol. 31, No. 3, pp 4-9, July 1986.

Corjon, A., Stoessel, A., 'Three-Dimensional Instability of Wake Vortices Near the Ground', 28th AIAA Fluid Dynamics Conference, June 29-July 2, 1997, Snowmass Village, CO, AIAA 97-1782.

Klein, R., Majda, A., and Damodaran, K., 'Simplified Equations for the Interaction of Nearly Parallel Vortex Filaments', J. Fluid Mech, Vol. 288, 1995, pp 201-248.

Marshall, J., and Chen, H., 'Stability of a counter-rotating vortex pair immersed in cross-stream shear flow', AIAA Journal, Vol. 35, February 1997, pp 295-305.

Kantha, L., 'Empirical Model of Transport and Decay of Wake vortices Between Parallel Runways', Journal of Aircraft, Vol. 33, No. 4 July-Aug. 1996.

Robins R. E., and Delisi, D. P, 1988, 'Numerical Study of Vertical shear and stratification effects on the evolution of a vortex pair', AIAA Journal, 28, 661-669.

Spalart, P. R., and Wray A. A., 1996, 'Initiation of the Crow Instability by atmospheric turbulence', 78th AGARD-FDP Symp. 'The Character & Modification of wakes from Lifting Vehicles in Fluids', Trondheim, Norway, 20-23 May 1996.

Schowalter, D. G., DeCroix, D. S., Switzer, G. F., Lin, Y.L. and Arya S.P., 'Toward Three-Dimensional Modeling of a Wake Vortex Pair in the Turbulent Planetary Boundary Layer', 5th Aerospace Sciences Meeting & Exhibit, Jan 6-10, 1997, Reno, NV, AIAA 97-0058.

Sarpkaya, T., 'Trailing Vortices in Homogeneous and Density Stratified Media', J. Fluid Mechanics, vol. 136, pp 85-109, 1983.

Rogers, S. E. 'Progress in High-Lift Aerodynamic Calculations', 31st Aerospace Sciences Meeting & Exhibit, Jan 11-14, 1993, Reno, NV. AIAA-93-0194.

Spalart, P. R., 'Airplane Trailing Vortices', to appear Annual Review of Physics, 1997.

Souders, W.G., Platzer, G.P. 'Tip Vortex Cavitation Characteristics and Delay of Inception on a Three-Dimensional Hydrofoil', DTNSRDC-81/007.

Eca, L., Falcao de Campos, J.A.C., Hoekstra, M. 'Prediction of Incompressible Tip Vortex Flows', 20th Symposium on Naval Hydrodynamics. 1994.

Hoeijmakers, H.W.M., 'Vortex Wakes in Aerodynamics', AGARD Conference on 'The Characterization & Modification of Wakes from Lifting Vehicles in Fluids', May 1996, Trondheim, Norway.

Kenwright, D. and Haimes, R., 'Vortex Identification - Applications in Aerodynamics: A Case Study, to be presented at .... (1997).

Kim, J., and Moin, P., 'The Structure of the Vorticity Field in Turbulent Channel flow, Part 2. Study of Ensemble Averaged Fields', J. Fluid Mechanics, 162, pp 339, 1986.

Villasenor, J., and Vincent, A., 'An Algorithm for Space Recognition and Time Tracking of Vorticity Tubes in Turbulence', CVGIP: Image Understanding 55:1, pp 27, 1992.

Globus, A., Levit, C., and Lasinski, T., 'A tool for Visualizing the Topology of Three-Dimensional Vector Fields', Report RNR-91-017, NAS Applied Res, Office, NASA Ames Research Center, 1991.

Banks, D., C., and Singer, B., A., 'A Predictor-Corrector Scheme for Vortex Identification', ICASE Report No. 94-22, NASA CR-1 94900, 1994.

Jeong, J., and Hussain, F., 'On the Identification of A Vortex', J. Fluid Mech., 285, pp 69-94., 1995.

## **Appendix: The Characterization of Wake Vortex Flows**

### **BACKGROUND:**

- The study of wingtip vortices is of great importance in many areas in fluid engineering and aeronautics. Tip vortices generated by wings on a large aircraft have been known to affect other aircraft following at a close distance. The blade/vortex interaction on rotorcraft blades is another area of interest since this interaction can directly affect the rotorcraft performance.

### **MOTIVATION**

- Although there has been a great deal of work done on tip vortex flows in the form of theoretical, experimental and computational studies, the current understanding of the details of the tip vortex flows have not been fully addressed. Details of the formation, growth and decay processes are not well understood. Mutual experimental/computational validation procedure is also lacking.

### **OBJECTIVE:**

- The overall objective is a detailed and systematic study of the development of the tip vortex on the wing, its convection and decay in the near- and intermediate fields behind wings.

### **I. TIP VORTEX FORMATION ON THE WING AND IN THE NEAR-FIELD**

**Collaborators: Greg Zilliac (FML), Jim Chow (Stanford U.), Dochan Kwak (ADC Branch) and Peter Bradshaw (Stanford U.)**

- In this region, the flow is highly turbulent and large gradients of pressure and velocity in all three directions are present which makes this computationally challenging. The vortex is formed at the tip which is fed by the vorticity from the boundary layer near the tip. As it travels downstream it roll-up more and more of the high momentum fluid from the boundary layer. A schematic of the development of a turbulent wingtip vortex at a moderate angle of attack is shown in Fig. 1.

### **Motivation:**

- Correct vortex decay rate not being predicted
- Poor turbulence modeling of the vortex.
- Uncertainty in physics of wingtip vortex development.

### **Goal:**

- Quantify to what extent numerical errors and turbulence modeling errors affect the accuracy of tip vortex flow prediction.
  - What is the grid requirement needed to resolve the high gradients?
  - What kind of turbulence modeling is needed to describe the tip vortex flow?
  - Can we isolate the turbulence modeling errors from the errors due to numerics?

- Provide some guidelines in properly resolving the tip vortex computations.

#### **Approach:**

- The approach to this study is slightly different from most studies in that the experiment and computation have progressed in parallel and in a highly interactive fashion with substantial integration of the experimental data into the computation. This approach is beneficial since the experiment can aid the computation by providing necessary boundary conditions for the computations but also, the computation can provide the experimentalist some information that may be difficult or time consuming to obtain in the lab. (Example, surface oil flow or skin friction values can be postprocessed from the computation which can help the experimentalist with the measurements).
- A three-dimensional, steady, and incompressible Navier-Stokes flow solver, INS3D-UP, was used in this study. Third-order and fifth-order upwind-biased finite-differencing scheme for the convective and pressure terms are studied.
- Two one-equation turbulence models have been studied; the Baldwin-Barth model and the Spalart-Allmaras model. These two models have been used with the production term modified to account for the stabilizing effect of the nearly solid body rotation in the vortex core.
- Grid refinement study using 0.6 million, 1.1 million, 1.5 million and 2.5 million grid points was performed.

#### **Accomplishments:**

- Out of this study, some guidelines in resolving the tip vortex flow in the formation, growth and decay stages have been accomplished. (See Table 1). Proper resolution of the vortex core properties (viscous vortex core radius and mean flow gradients) in the wake region, was achieved by refining the crossflow plane using 23-26 points in the viscous vortex core. Grid refinement in the axial direction was not as sensitive as the crossflow plane refinement. An average of 35 points in the axial direction was adequate to achieve proper convection of the vortex  $0.75c$  in the wake region. In addition, a  $y^+$  between 0.16 and 0.36 is recommended in order to properly resolve the boundary layer. This is contrary to the prescribed  $y^+$  of about 1.0.
- Useful observations and results of the solution of the tip vortex flowfield for 4 grid sizes were obtained. The maximum difference between experiment and computation is found in the core-centerline values (table 1). It is interesting to note that for the 1.5 million grid size, it is possible to obtain a reasonable prediction of the core axial velocity yet significantly underpredict the pressure. This comparison was the poorest of the quantities studied. In order to see if numerical error is still present at this stage, further grid refinement using 2.5 million grid points was done. When the crossflow plane was refined one and one-half times the grid size in the core vicinity, improvement in the comparison is observed with a 3% error in the velocity and 11% error in the static pressure.
- Although grid independence is not yet reached with the finest grid, the lift and drag



coefficients do not change that much between the two fine grids (less than 0.2 %). However, the difference between the measured values of  $C_l$  and the computed  $C_l$  using 2.5 million grid calculation is 7.6%. The measured  $C_l$  values were obtained by integrating the  $C_p$  distribution and are not considered to be very accurate owing to insufficient number of points (pressure taps) used in the integration process (Table 2).

- Good agreement with measured results was found using 1.5 million grid points and finer, and using the modified turbulence models. Velocity profiles through the vortex compared to within 3% of the experiment. The occurrence of a secondary vortex has also been compared. (See Fig.2 for the experiment/computation set-up and the velocity magnitude comparisons).
- The artificial spreading of a vortex caused by the numerical dissipation errors has been successfully addressed. Fifth-order accurate upwind-biased differences of the convective terms was found to be essential in reducing numerical dissipation and achieving reasonable agreement with measured vortex velocity profiles (Fig. 3). The underprediction of the flow quantities in the core region is thought to be caused by turbulence modeling. On the wing surface, the extent of the turbulence modeling error and numerical errors are yet to be quantified.
- This study found that both the Baldwin-Barth one-equation model and the Spalart-Allmaras one-equation model in their original form, are not adequate for accurate tip vortex flow prediction. An ad-hoc modification of the production term for both models was needed to account for the stabilizing effect of the nearly-solid body rotation of the core of the vortex. (See Fig. 4 for comparison of the two turbulence models with experiment). However, the fact that the principal axes of the Reynolds stress and mean strain rate tensors are not aligned suggests that an eddy viscosity approach (constant or isotropic) will most likely be not fully successful in resolving tip vortex flows. In addition, we showed that the resolution of the viscous vortex core properties are dependent not only on the core circumferential velocity distribution but also on the turbulent stress terms in the near-field of a wing tip. This needs to be studied further.
- In the wake region, excellent comparison is obtained outside of the viscous vortex core. In the viscous core region, the viscous vortex core size was predicted to within one to two percent of the experiment; the velocity magnitude right on the centering of the viscous vortex core was predicted to within three percent while the static pressure coefficient was predicted to within 11 percent. On the wing surface, a similar trend is observed but a bigger discrepancy was observed around the viscous vortex core region. Note that around this area where the vortex is still forming, the core region is not fully defined. As a result, the core is harder to quantify and a detailed vortex core-centering comparison is hard to make.
- This study attempted to quantify to what extent numerics and turbulence models affect the accuracy of tip vortex flow prediction. We found that for a minimum grid size of 1.5 million grid points (single grid approach), the error from numerics and the 'error' contributed by the turbulence models are of the same order of magnitude and so their

separate contribution to the inaccuracy of the solution was not quantifiable. Refining the grid further in the crossflow plane to obtain a total of 2.5 million grid points improve the comparisons between computation and experiment in all three stages of development. This suggests that we were successful in reducing the numerical errors compared to turbulence modeling errors.

### **Future Plans**

- Investigate the role of adaptive gridding to expedite grid generation process and to reduce the total grid points needed to resolve the high gradients.
- Improve the prescription of the outflow boundary condition
- Obtain a more general turbulence modeling modification for tip vortex flows.

## **II. WAKE VORTEX PROPAGATION IN THE NEAR- FIELD**

**Collaborators: Dochan Kwak(ADC Branch) and Mohamed Hafez (U. C. Davis)**

- In the near-wake region, the tip vortex continues and completes the roll-up process. This region extends to up to 5-6 wing spans downstream of the trailing edge.(Note that a commercial wingspan is about 200 ft).Trailing vortices can persist for several miles downstream of a lifting surface. As it travels downstream, it undergoes several physical changes which are complicated not well understood (See figs. 1 and 5). Some of the characteristics of the near-wake which are still not well understood are:
  - when does the u-velocity excess becomes a deficit, what influence does it have on the strength of the vortex?
  - does the vortex re-laminarizes within this region?
  - what influence does turbulence have in the roll-up process and how can this be modeled in a less 'ad-hoc' procedure?

### **Motivation:**

- Most flow prediction model the wake region where the vortex has been assumed to have completed its roll-up process which is in the intermediate wake. But it is equally important to model the initial vortex formation/roll-up process and the near-wake for accurate drag prediction.

### **Goal:**

- Given some knowledge of the tip vortex formation on the wing and in a short portion of the near-field (less than  $0.75c$ ), obtain some insights into a more physical wake modeling by including the viscous upstream effects and other physics.
- Investigate the validity and applicability of the velocity-vorticity formulation of the Navier-Stokes equations as a possible candidate for wake modeling.

- Investigate the efficiency of INS3D-UP with adaptive gridding in solving that part of the near-wake when wake modeling might not be fully applicable, i.e, flow is still fully turbulent and three-dimensional.
- Provide an improved vortex flowfield to be used as inflow for the intermediate-wake.

#### **Approach:**

- Validate the velocity/vorticity solver and the model using analytical vortices which represents a near-field behavior(3-D Burgers vortex), and an intermediate-field behavior (Perturbed vortex).

#### **Solution Methods:**

##### **I. Velocity/Vorticity Formulation:**

- preserves accuracy by using vorticity as the working variable.
- compact scheme, allows use of first-order differencing without sacrificing accuracy
- allows flexibility in incorporating measured results as b.c.'s.

##### **Model I. Stream function/Vorticity**

- quasi-two dimensional
- ideal-wake assumption allows use of parabolic marching scheme.
- streamwise u-velocity constant
- regular grid arrangement
- no turbulence modeling

##### **Model II: Velocity/Vorticity Model**

- quasi-two dimensional
- ideal-wake assumption allows use of parabolic marching.
- stretching terms for vorticity in the y- and z- directions negligible.
- streamwise u-velocity allowed to vary
- staggered grid arrangement for more compactness
- no turbulence modeling

##### **II. INS3D-UP + adaptive gridding**

- fully vectorized and optimized.
- efficient and accurate using 5th-order scheme
- turbulence models exists already to handle tip vortex flows
- outflow b.c. needs to be fixed

#### **Accomplishments:**

Since work on this topic is less than a year old and is still on-going, the results are still preliminary and most of the work is yet to be done.

- Explored the validity of the velocity/vorticity formulation and preconditioned conjugate gradient method.
- Demonstrated the capabilities of the stream function/vorticity model (Model I) and the velocity/vorticity model (Model II) in predicting wake-vortex flow (Figs. 6 and 7).

**Current Work:**

- Improve the efficiency of Model II.
- Validate Model II for a near-wake case
- Assess the accuracy and efficiency of Model I and II.

**Future Plans:**

- Incorporate adaptive formulation techniques.
- Incorporate turbulence modeling for the velocity/vorticity methods.

**II. WAKE VORTEX PROPAGATION IN THE INTERMEDIATE- FIELD**

**Collaborators: Dochan Kwak(ADC Branch) and Mohamed Hafez (U. C. Davis)**

- In the intermediate wake the vortex is well established. This region usually extends from 6-7 to a few hundred wing spans behind a lifting surface. This region is very well studied with a wide range of wake modeling techniques. Most, if not all, of the modeling techniques assume a theoretical vortex profile (perturbed vortex, Lamb's vortex, etc.), as the inflow condition to start the calculation. Some of the issues yet to be resolved in this region are:
  - is the flow laminar or turbulent,
  - how do we incorporate freestream turbulence
  - is the u-velocity distribution still important
  - how important is the viscous upstream effect
  - does the vortex meander

**Goal:**

- Provide a wake model with a more physical foundation.
- Investigate Model I and II used for the near-wake case as possible candidates to model the intermediate-field.
- Incorporate effect of freestream turbulence.

**Approach:**

- Validate the intermediate region using measured data (Rossow et al, 1993). The measured data used for comparison was taken at the 80 x 120 foot wind tunnel at NASA Ames Res. Center, which are though to be the best data available to date. The wake generating model was that of a 0.03 -scale model of the B-747 at  $Re = 6.6 \times 10^5$ .
- Obtain other experimental results to validate the code.

**Solution Methods using Velocity/Vorticity:****Model I. Stream Function/Vorticity Model**

- (same as in the near-wake case)
- code is efficient but needs to compare with some other wake models.

**Model II. Velocity/Vorticity Model**  
- (same as in the near-wake case)

**Accomplishments:**

Since work on this topic is less than a year old and is still on-going, the results are still preliminary and most of the work is yet to be done.

- Comparison with measured data of the 0.03 scale model of the Boeing 747, taken at the 80- by 120 foot wind tunnel (Rossow, et al), showed a similar trend between the measured and computed up- and down-wash velocity. The slopes of the velocity across the vortex was predicted well by the computation (which was previously missed by other wake models found in literature). Most of the disagreement is in the region where the sampling period of the measured data was not long enough which resulted in the jaggedness of the data.(Fig. 8)
- Full Navier-Stokes solution is very similar to Model II which suggests that for the flow tested, most of the physics obtained by using the full N-S solver is retained which makes Model II a good candidate for wake modeling. Notice also that the slope of the velocity across the vortex core is less steep using Model I but the overall feature is well preserved.(Fig. 9).

**Current Work:**

- Perform an efficiency comparison between existing wake models such as the vortex lattice method, vorticity confinement method, with Models I and II.

**Future Plans:**

- Adaptive gridding
- Include freestream turbulence modeling

## List of Tables and Figures:

Figure 1. Development of a Turbulent Wingtip Vortex

Table 1: Effect of Grid Refinement and Turbulence Models ( $x/c=1.241$ )

Table 2: Tabulated Values of Computed Lift and Drag Coefficients.

Figure 2. Wingtip Validation Study.

Figure 3 Comparison of third-order and fifth-order differencing schemes, and modified and unmodified production term of the one-equation Baldwin-Barth turbulence model.

Figure 4. Comparison of crossflow velocity contours at  $x/c=0.813$  using the BB model and the SA model. Also shows effect of refining the grid on the SA model.

Figure 5. Model of the wake downstream of a lifting wing of finite span.

Figure 6. Model I: Stream Function/Vorticity Formulation.

Figure 6a. Comparison of convergence history for Symmetric Gauss-Seidel (SGS), Conjugate Gradient (CG), and Preconditioned Conjugate Gradient(PCG) Methods.

Figure 6b. Streamwise propagation of the X-component of the vorticity across the vortex core.

Figure 7. Model II: Velocity/Vorticity Formulation.

Figure 7a. Comparison of the convergence history for SGS and PCG methods.

Figure 8. Comparison with measured data using the full N-S solver.

Figure 8a. W-velocity distribution as it propagates in the x-direction.

Figure 8b. Comparison of the up- and down-wash velocity profile with measured data at  $x/c=162$  ft.

Figure 9. Comparison of the measured data with the full N-S solution, Model II and Model I.

**Table 1: Effect of Grid Refinement and Turbulence Models ( $x/c=1.241$ )**

| Grid Size              | $ V $ at vortex core centerline | Max. Crossflow Vel near core | Min. $C_p$ Static at core centerline | Comments  |
|------------------------|---------------------------------|------------------------------|--------------------------------------|---|
| 0.6 million (BB model) | 1.03                            | 0.55                         | -0.60                                | Vortex highly diffused with no peak velocity seen.  |
| 1.1 million (BB model) | 1.31                            | 0.91                         | -1.32                                | Peak velocity not clearly observed.   |
| 1.5 million (BB model) | 1.72                            | 0.980                        | -2.73                                | B.L. resolved, wake topology modified, grid improved. Peak velocity resolved well, vortex symmetric in shape.                         |
| 1.5 million (SA model) | 1.70                            | 1.06                         | -2.77                                | Similar behavior as BB but more detailed features of the vortex are observed (e.g. detailed account of the wrapping around of fluid). |
| 2.5 million (SA model) | 1.799                           | 1.02                         | -3.10                                | Crossflow plane refine 1.5 x previous grid.   |
| Experiment             | 1.75                            | 0.93                         | -3.51                                |   |

**Table 2: Tabulated Values of Computed Lift and Drag Coefficients**

| Grid Size <sup>a</sup>                | $C_D$  | $C_L$ |
|---------------------------------------|--------|-------|
| 2.5 million grid points (115x189x115) | 0.1624 | 0.512 |
| 1.5 million grid points (115x157x83)  | 0.1620 | 0.513 |
| 1.1 million grid points (103x145x73)  | 0.1448 | 0.435 |
| 0.6 million grid points (83x130x53)   | 0.1267 | 0.405 |
| Experiment                            | -----  | 0.51  |

**Figure 1. Development of a Turbulent Wingtip Vortex**





# WINGTIP VORTEX VALIDATION STUDY

INS3D-UP, NACA0012,  $Re=4.6$  million,  $AOA=10$  degrees

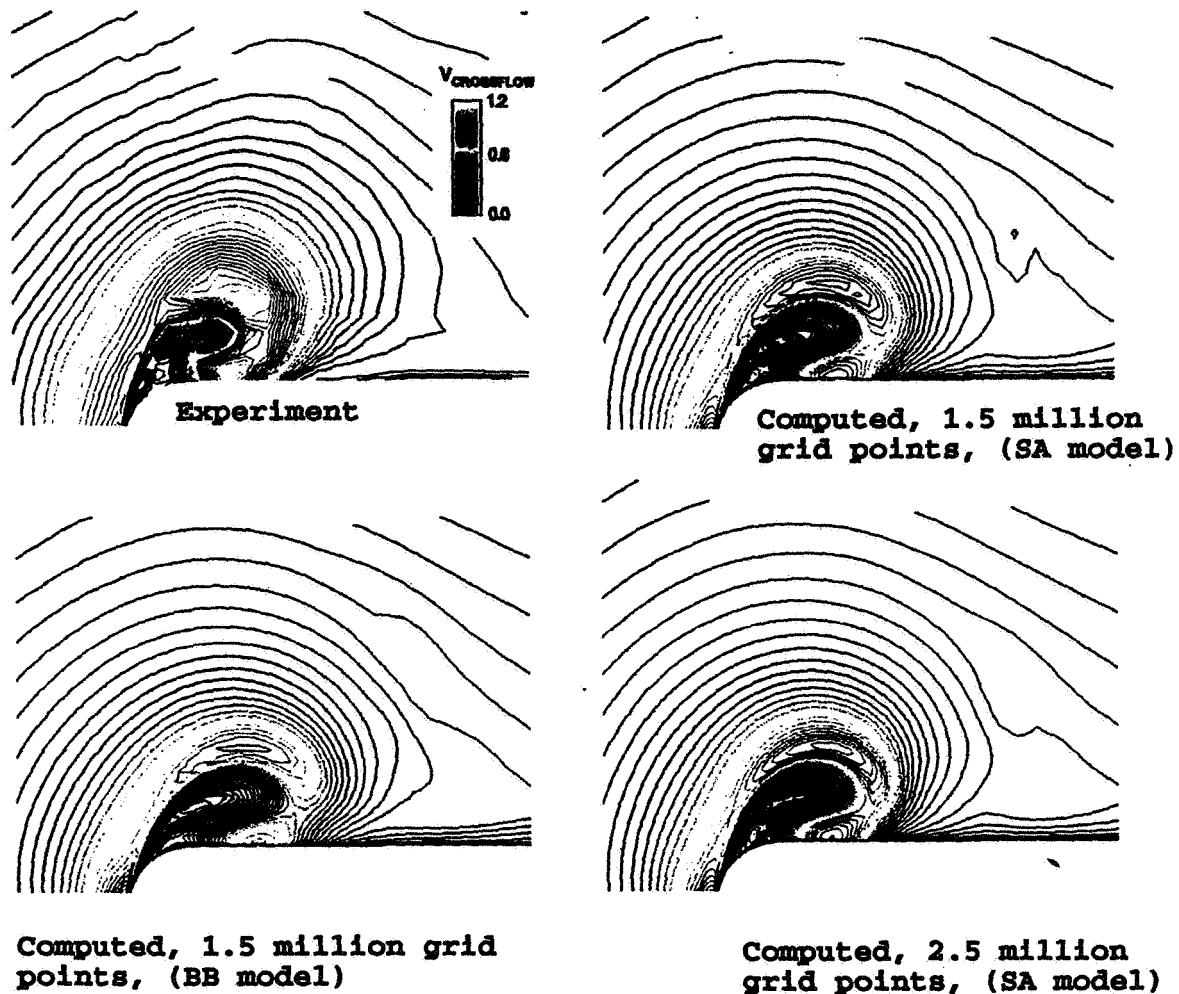


Fig. 4 Comparison of crossflow velocity contours at  $x/c=0.813$  using the BB model and the SA model. Also shows effect of refining the grid on the SA model.

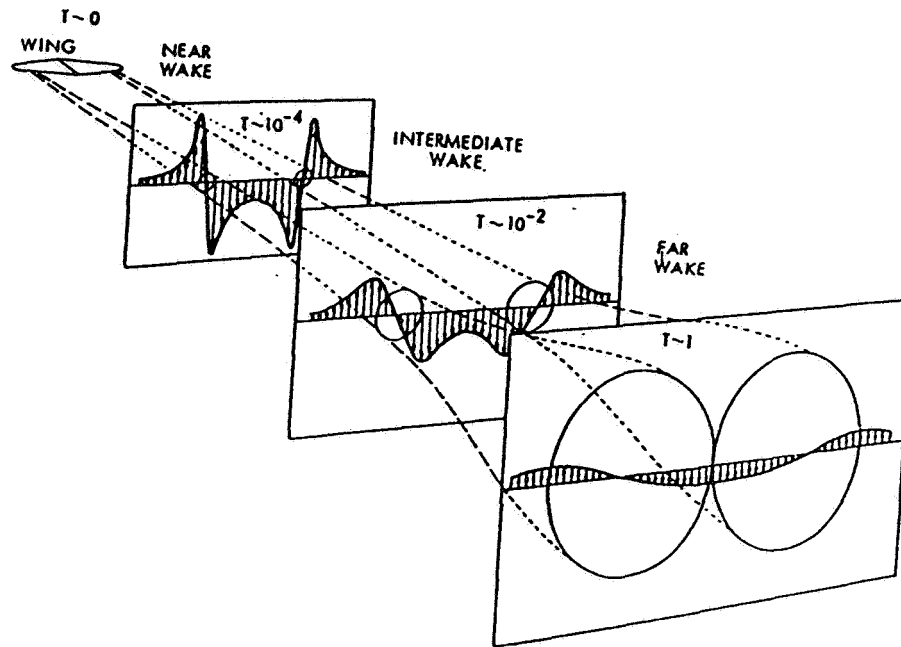


Figure 5. Model of the wake downstream of a lifting wing of finite span.

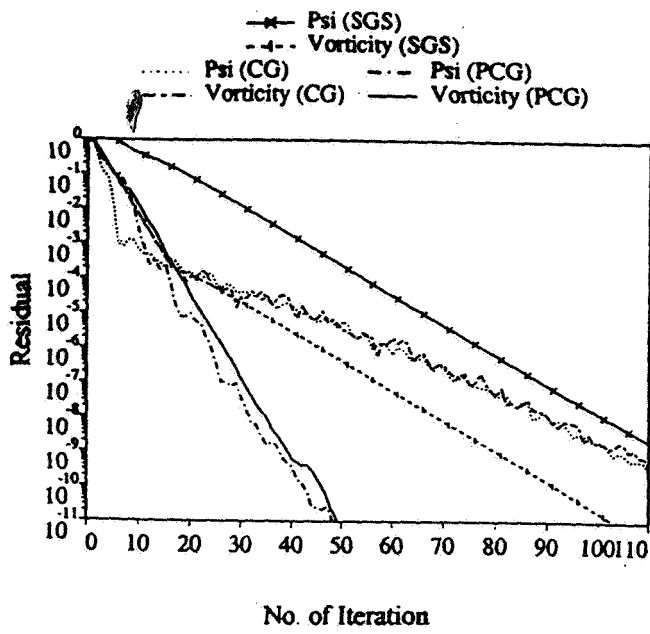


Figure 6a. Comparison of convergence history.

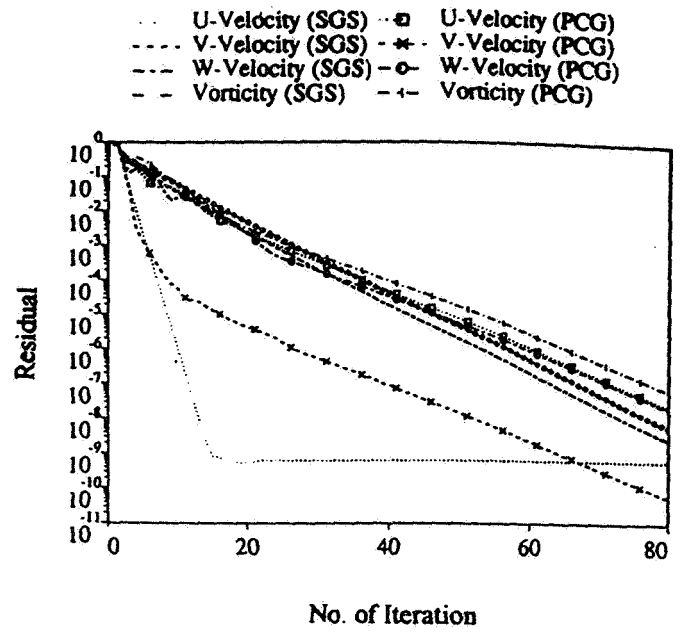


Figure 7a. Comparison of the convergence history.

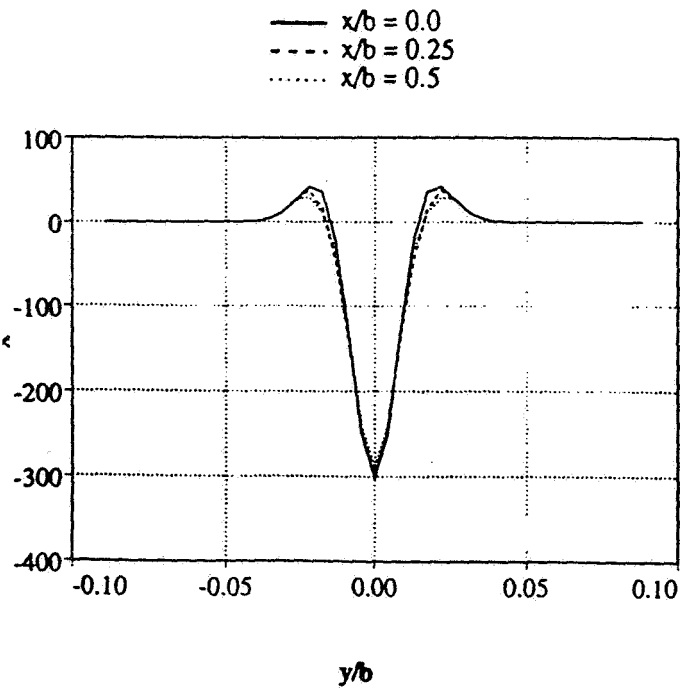


Figure 6b. Streamwise propagation of the X-component of the vorticity across the vortex core.

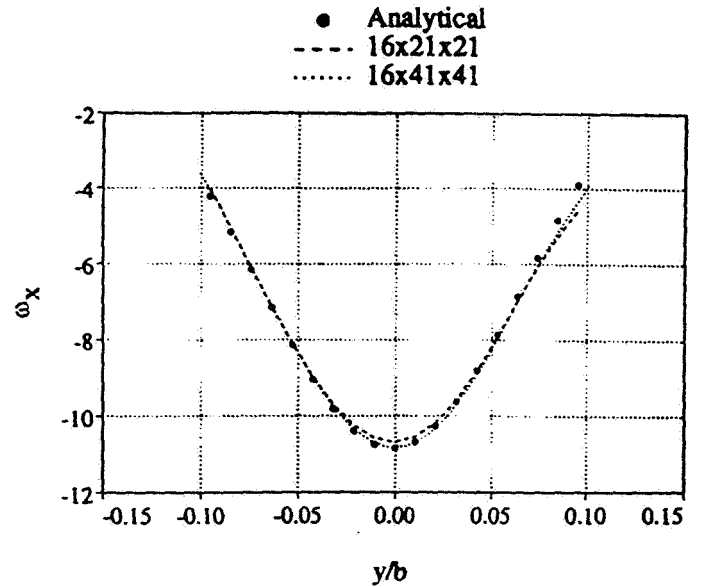


Figure 7b. X-component of the vorticity across the vortex core.

Figure 6. Model I: Stream Function/Vorticity Formulation.

Figure 7. Model II: Velocity/Vorticity Formulation.

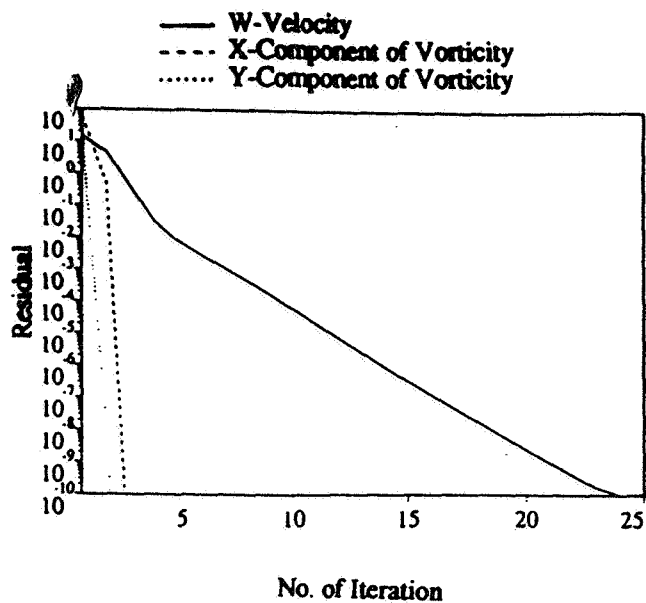


Figure 8a. Convergence history.

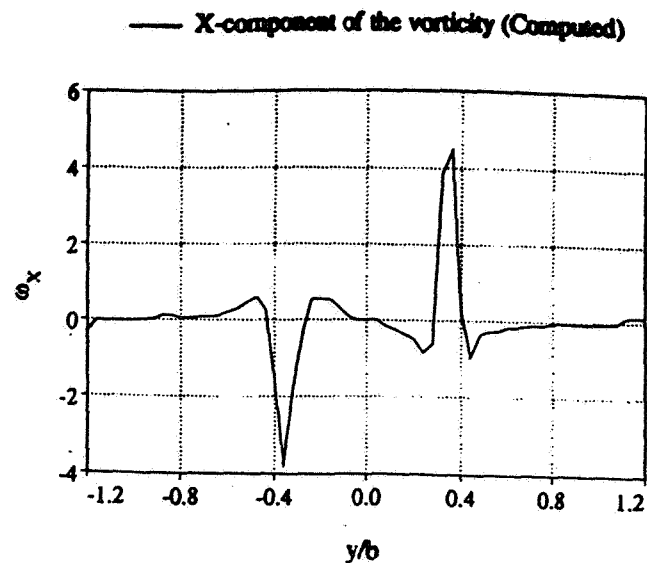


Figure 8c. X-component of the vorticity across the vortex pair at  $x/c=162$  ft.

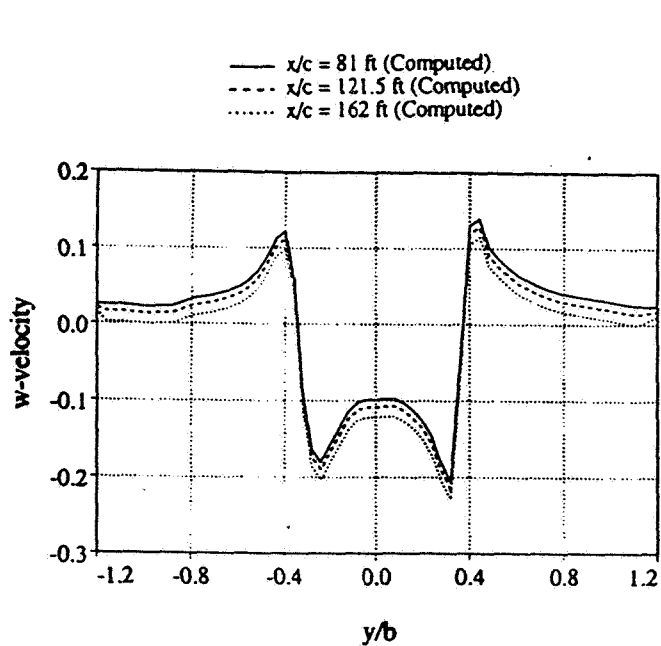


Figure 8b. W-velocity distribution as it propagate in the x-direction.

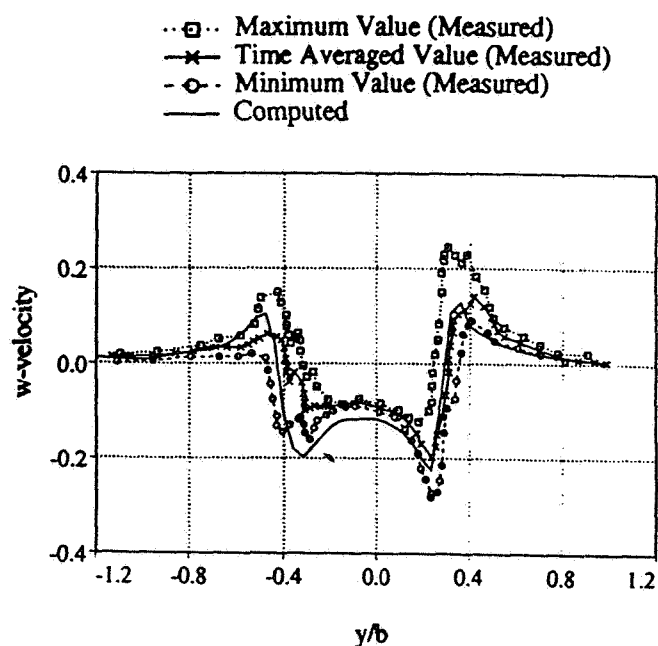


Figure 8b. Comparison of the up- and down-wash velocity profile with measured data at  $x/c=162$  ft.

Figure 8. Comparison with measured data using the full N-S solver.

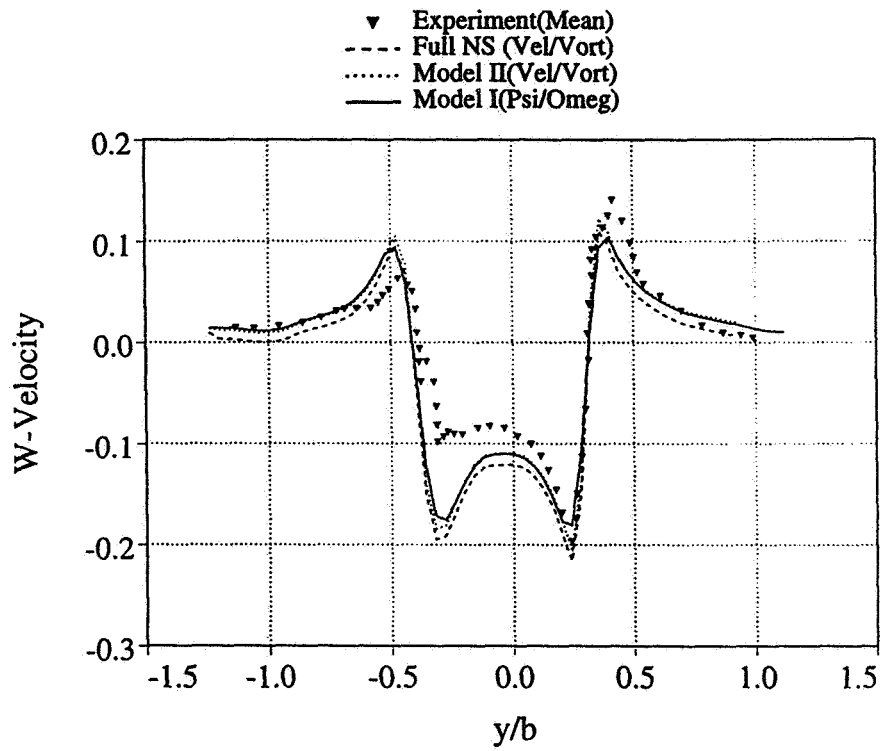
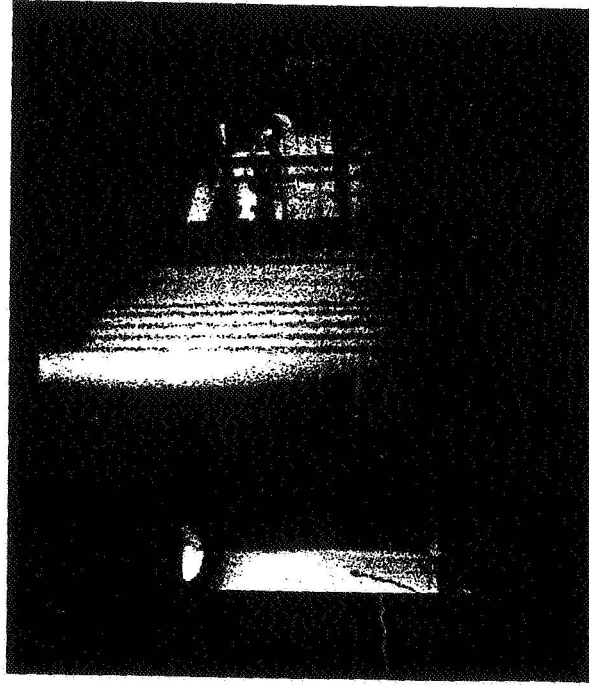


Figure 9. Comparison of the measured data with the full N-S solution, Model II and Model I.

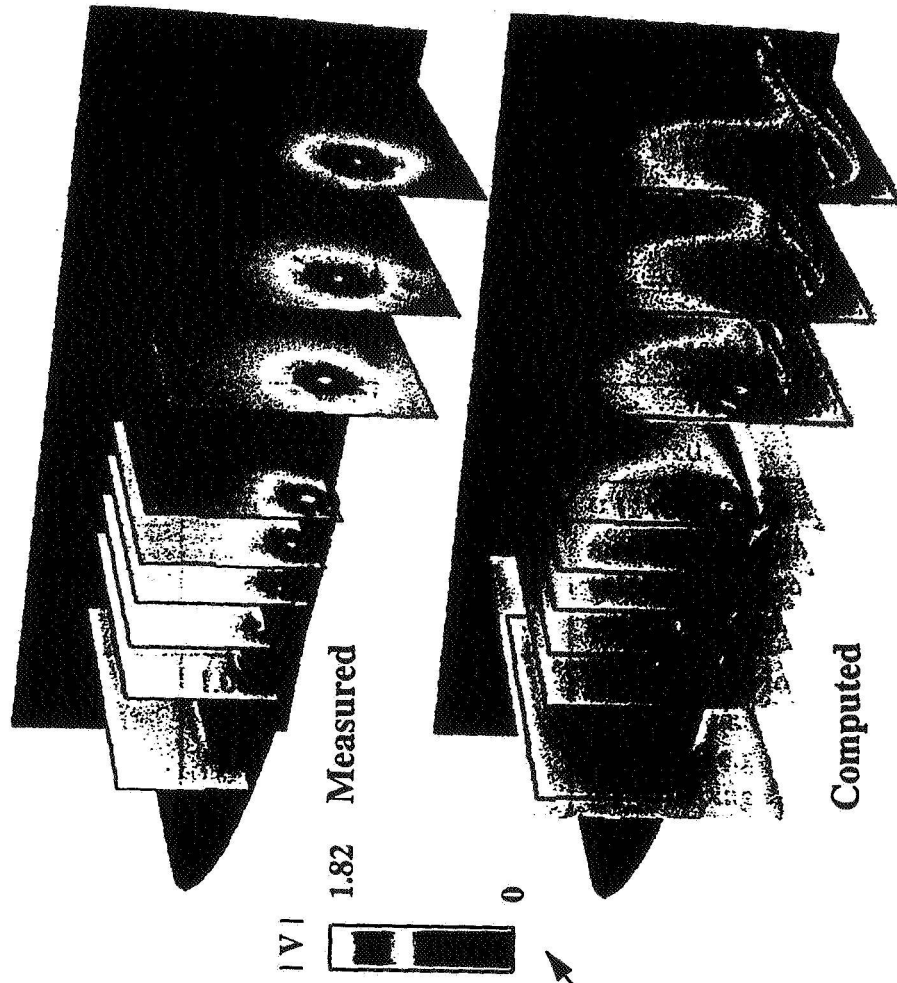
# WINGTIP VORTEX VALIDATION STUDY

INS3D-UP CODE, NACA0012,  $Re = 4.6e6$ ,  $\alpha = 10^\circ$ , GRID SIZE =  $115 \times 157 \times 83$

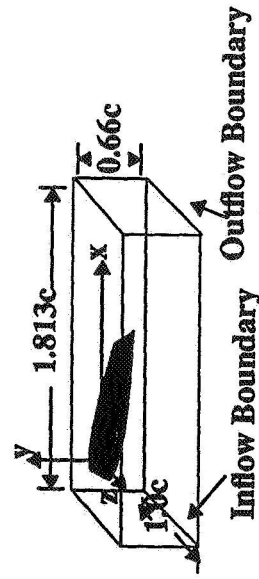
32 in. x 48 in. FML Wind Tunnel



Velocity Magnitude Comparison between Exp. and Computation



Computed/Measured Domain



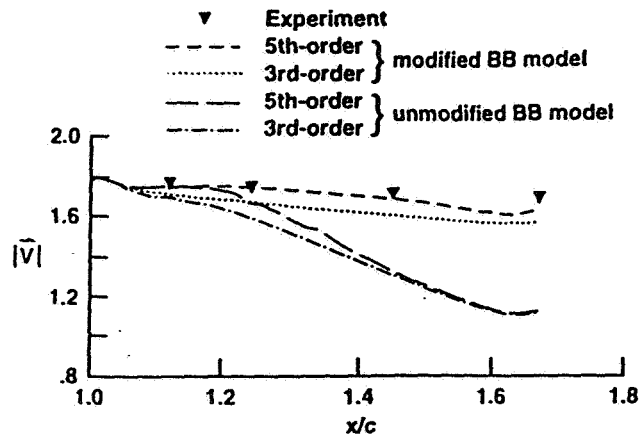


Fig. 3a Peak velocity magnitude at vortex core.

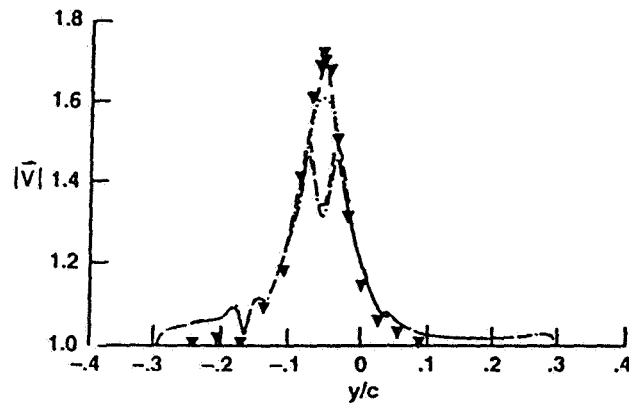


Fig. 3b Total velocity magnitude across vortex core at  $x/c = 1.241$ .

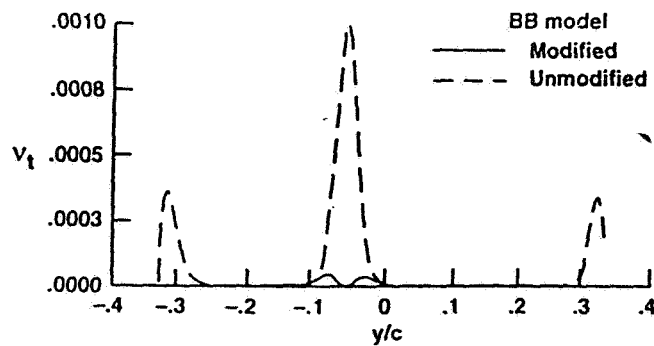


Fig. 3c Eddy viscosity profile across vortex core at  $x/c = 1.241$ .

Figure 3 Comparison of third-order and fifth-order differencing schemes, and modified and unmodified production term of the one-equation Baldwin-Barth turbulence model.

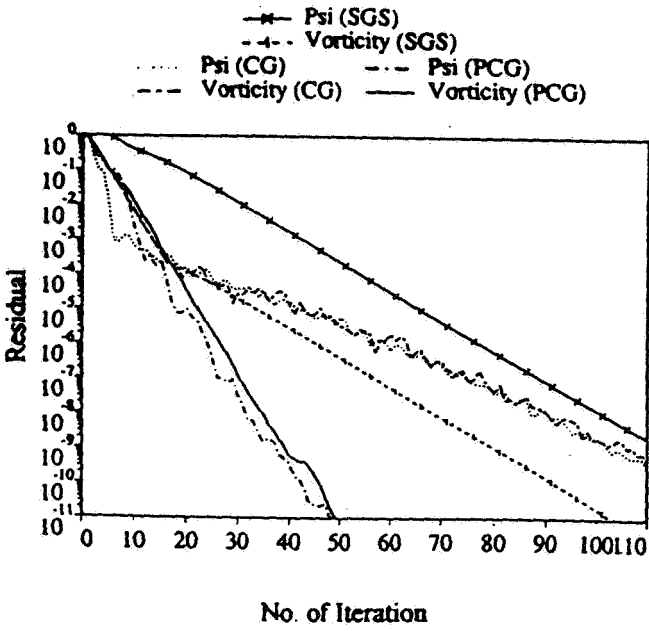


Figure 6a. Comparison of convergence history.

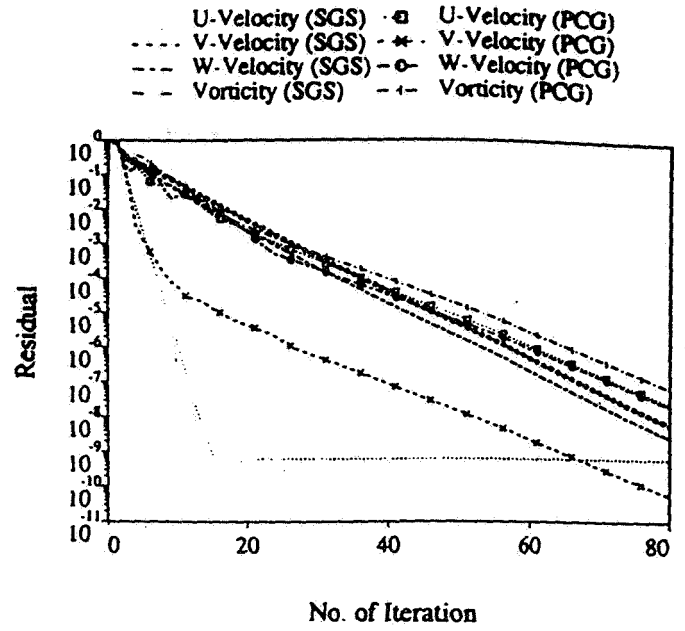


Figure 7a. Comparison of the convergence history.

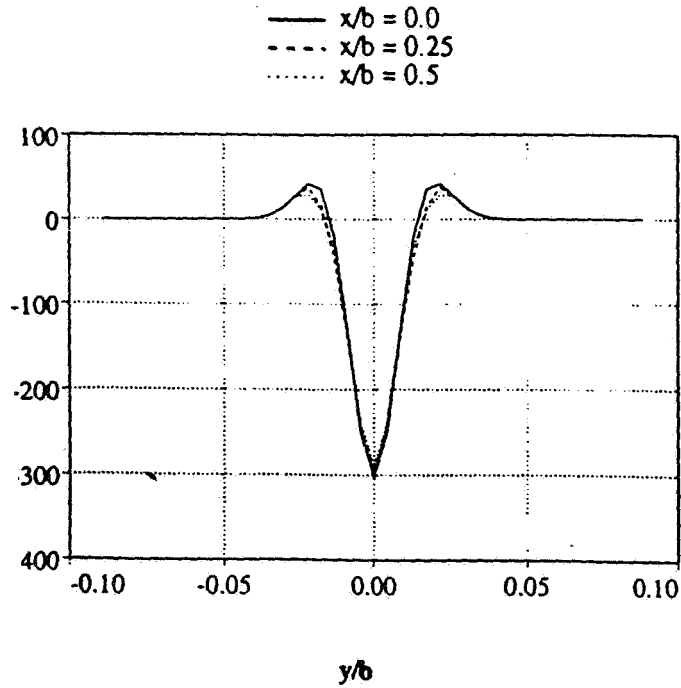


Figure 6b. Streamwise propagation of the X-component of the vorticity across the vortex core.

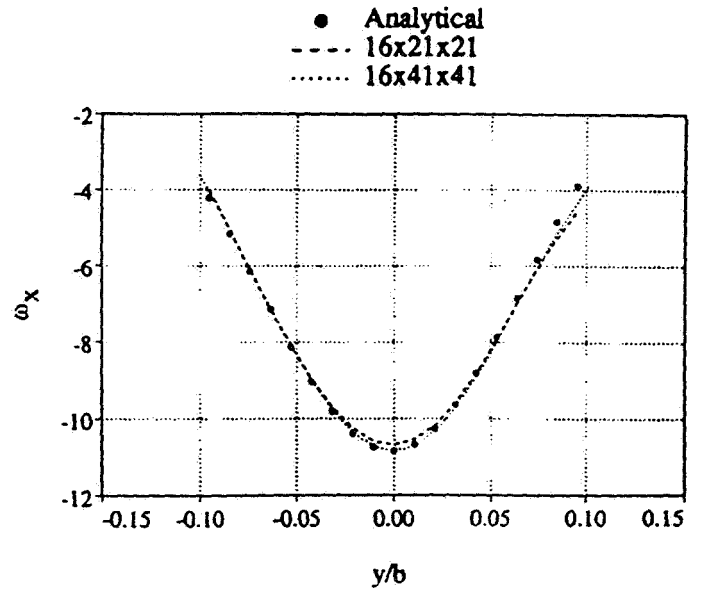


Figure 7b. X-component of the vorticity across the vortex core.

Figure 6. Model I: Stream Function/Vorticity Formulation.

Figure 7. Model II: Velocity/Vorticity Formulation.



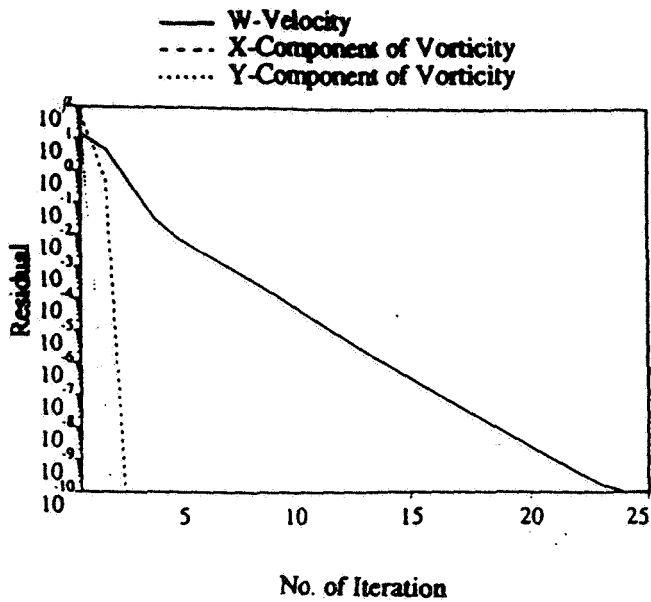


Figure 8a. Convergence history.

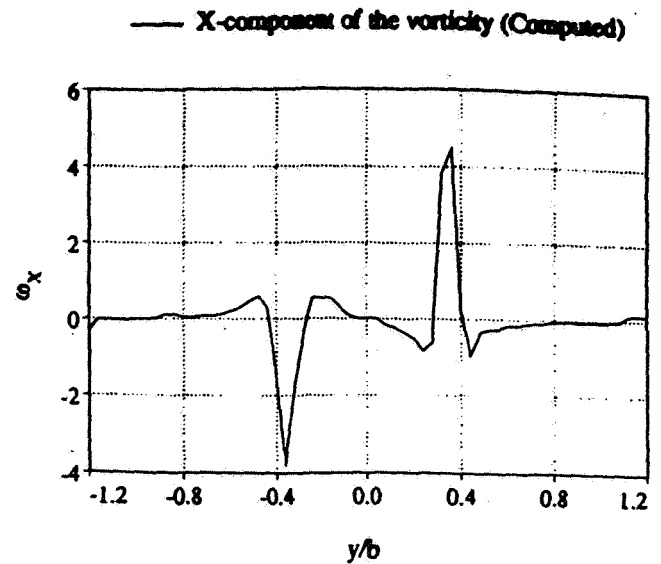


Figure 8c. X-component of the vorticity across the vortex pair at  $x/c=162$  ft.

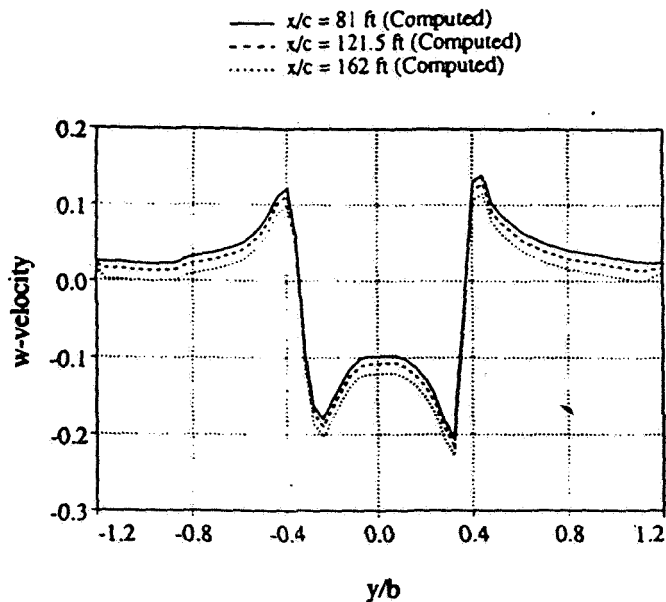


Figure 8b. W-velocity distribution as it propagate in the x-direction.

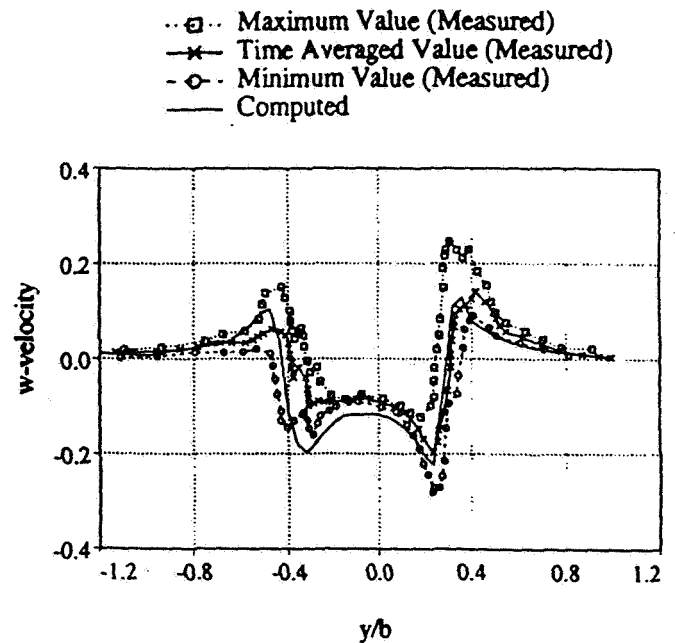


Figure 8b. Comparison of the up- and down-wash velocity profile with measured data at  $x/c=162$  ft.

Figure 8. Comparison with measured data using the full N-S solver.

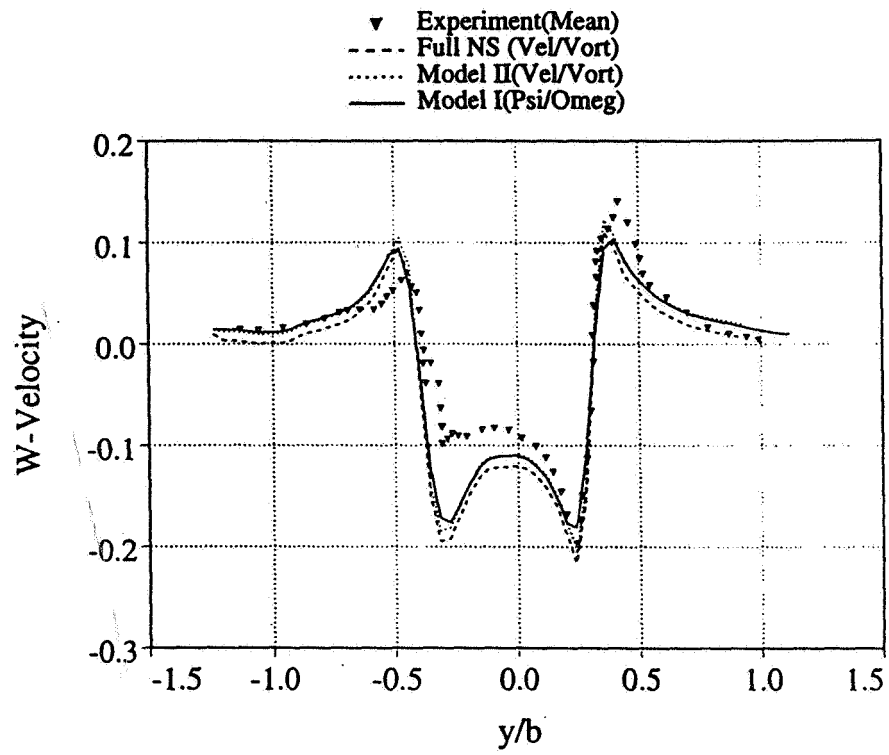


Figure 9. Comparison of the measured data with the full N-S solution, Model II and Model I.